DEPARTMENT FOR INNOVATION IN BIOLOGICAL, AGRO-FOOD AND FOREST SYSTEMS - DIBAF
Università degli Studi della Tuscia
Via S. Camillo de Lellis ,01100 Viterbo, Italy

MSc THESIS

MSc course: "Forestry and Environmental Sciences" (Classe LM-73)
International Curriculum with Multiple Diplomas – Specialization:
«Mediterranean Forestry and Natural Resources Management - MEDfOR»

ASSESSING BIODIVERSITY RELATED VARIABLES BY UNMANNED AERIAL VEHICLE (UAV) REMOTE SENSING

SUPERVISOR: Prof. BARBATI Anna

CANDIDATE: BAGARAM Bawinabadi
Matr. 199

CO-SUPERVISOR: Dr. GIULIARELLI Diego

ACADEMIC YEAR 2016/17

DOUBLE DIPLOMA ISSUED IN COLLABORATION WITH

MEDfOR
European Erasmus Mundus MSc

Erasmus Mundus

ABSTRACT

The continuous collection of forest data is crucial for a sustainable forest management. However, forest inventory data collection is time consuming and expensive. Remotely sensed data appear as an alternative to the field inventory. Despite the general knowledge of advantages satellite and airborne remote sensed data present, they possess a limitation in the application of forest management inventories and small-scale forest monitoring where a number of forest stand structural, compositional variables must be assessed at extremely fine spatial scales. The unmanned aerial vehicles (UAV) imagery could be used to overcome the limitation the satellite/airborne remote sensing presents.

This research explored the capability of a UAV, namely the eBee drone, imagery to map forest canopy gaps and derive some forest parameters such as, biodiversity indices, habitat trees, basal area, canopy height, deadwood, etc. using handy techniques in a test area of 240 ha of natural reserve of Lago di Vico in Central Italy. We used correlation and linear regression techniques to explore relationships between gaps patch metrics on one side and forest features on the other.

The mapping revealed that forest shaded canopy gaps can be faithfully extracted from UAV true color images. Estimation of forest features using canopy gaps as a proxy led to disparate results. Best results were obtained for understorey data with R^2 going up to 0.87 and intermediate results were observed in living trees data with R^2 of over 0.74. The approach failed to estimate the deadwood. Additionally, from the three forest types available in the study area, best results were observed in mixed forest while Fagus forest had the poorest ones and Quercus forest displayed intermediate results. UAV true color remote sensing presents a high potential for forest inventory, forest monitoring, and biodiversity assessment.

Keywords: Drones, high resolution images, forest gaps, diversity, habitat trees, spatialization, UAS

Acknowledgements

TABLE OF CONTENTS

TABLE OF FIGURES

LIST OF TABLES

GLOSSARY

a.s.l:	Above the Sea Level
ALS:	Airborne Laser Scanning
CBH:	Canopy Base Height
CHP:	Canopy Height Profile
DBH:	Diameter at Breast Height
DTM:	Digital Terrain Model
GPC:	Ground Control Points
GPS:	Global Positioning Systems
GSD:	Ground Sampling Distance
IMU:	Inertial Measurement Unit
KNN:	K-Nearest Neighbor
LAI:	Leaf Area Index
LDA:	Linear Discriminant Analysis
LiDAR:	Light Detection And Ranging
LS:	Laser Scanning
MD:	Mean absolute Deviation,
OOB:	Out Of the Bag error
RF:	Random Forest
RMSE:	Root Mean Square Errors
SfM:	Structure from Motion
SFM:	Sustainable Forest Management
SVM:	Support Vector Machines
SWIFT:	Scale Invariant Feature Transform
UAV:	Unmanned aerial vehicle

EXTENDED ABSTRACT

The continuous collection of forest data is crucial for a sustainable forest management. However, forest inventory data collection is time consuming and expensive. Remotely sensed data appear as an alternative to the field inventory. Despite the general knowledge of advantages satellite and airborne remote sensed data present, they present a limitation in the application of forest management inventories and small-scale forest monitoring where a number of forest stand structural (e.g. tree density, basal area, stand height, volume), compositional (e.g. dominant species, species proportions) or health status (e.g. crown condition) variables must be assessed at extremely fine spatial scales. In fact, these variables are usually collected on ground sample plots as large as 400-500 m^2. The unmanned aerial vehicles (UAV) imagery could be used to overcome the limitation the satellite/airborne remote sensing presents.

This research explored the capability of a UAV, namely the eBee drone, imagery to map forest canopy gaps and derive some forest parameters such as, biodiversity indices, habitat trees, basal area, canopy height, deadwood, etc. using handy techniques in a test area of 240 ha of natural reserve of Lago di Vico in Central Italy. We used correlation and linear regression techniques to explore relationships between gaps patch metrics on one side and forest features on the other.

To achieve those objectives, we firstly mapped forest canopy gaps using the contrast split algorithm based on the red band of the RGB orthomosaic. Secondly, we calculated for each gap the extent and shape metrics. Thirdly, we aggregated the data on plots' level by only assigning to each plot gaps that completely lie inside the plot or have over 50% of their area within the plot. Fourthly, for each plot, we calculated the mean, the standard deviation, the sum, the coefficient of variation associated with the patch metrics considering minimum area thresholds of 1 m^2 and 2 m^2, separetely. Sixthly, we performed statistical analyses on the collinearity among patch metrics and exploratory analysis for the field parameters which were grouped in three different datasets, namely, the understorey, the living trees and the deadwood. Seventhly, we performed the correlation and regression analyses on gap patch metrics and field parameters. Finally, for field parameters that led to an $R^2 > 0.5$ we produced the forest map of the parameter and using the cross-validation method, we produced the RMSE associated to each map.

The results showed that contrast split algorithm is effective in mapping forest canopy gaps, particularly the shaded gaps. The 95 patch metrics calculated for each plot (for each threshold) were highly collinear. In the study area, the three forest types (Fagus, Quercus and Mixed forests) do not have the same understorey, and the same characteristics of living trees but the deadwood distribution is roughly the same.

As a whole, the total deadwood volume presented a poor correlation with patch metrics. A similar result is obtained when the deadwood is separated either in decay class or in type of deadwood (eg. Standing deadwood, living deadwood, etc). For the understorey, the field parameters were strongly correlated with gap patch metrics. For instance, Shannon index and mean DBH in the Quercus forest yielded an $R^2 > 0.5$ while in Mixed forest, number of plants, mean HTOT and mean DBH exceeded that threshold (Fig1). Results were relatively lower in Fagus forest, with only Pielou index R^2 close to 0.5.
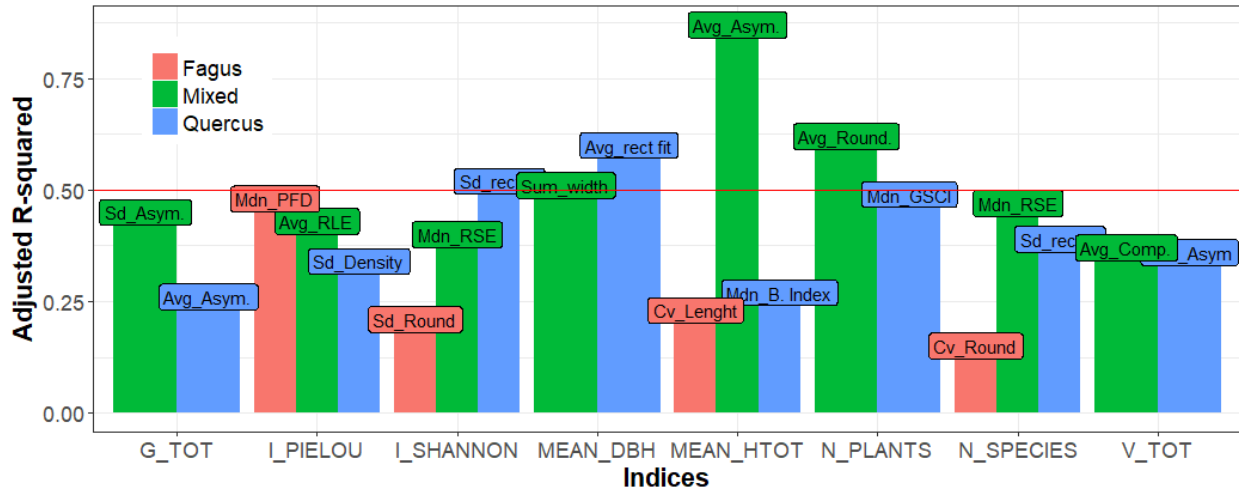
Fig1. Summary bar chart of adjusted R² from linear regression with understorey data in all the three forest types. On top of each bar, the gap patch metric used for linear regression

Results for the living trees (Fig2) were similar to the ones in the understorey. We found strong correlations between gap patch metrics and living trees parameters. In addition to the DBH and HTOT, Pretzsch index, which is an indicator of vertical structure complexity and habitat trees, which is a functional diversity indicator, depicted all $R^2 > 0.5$.
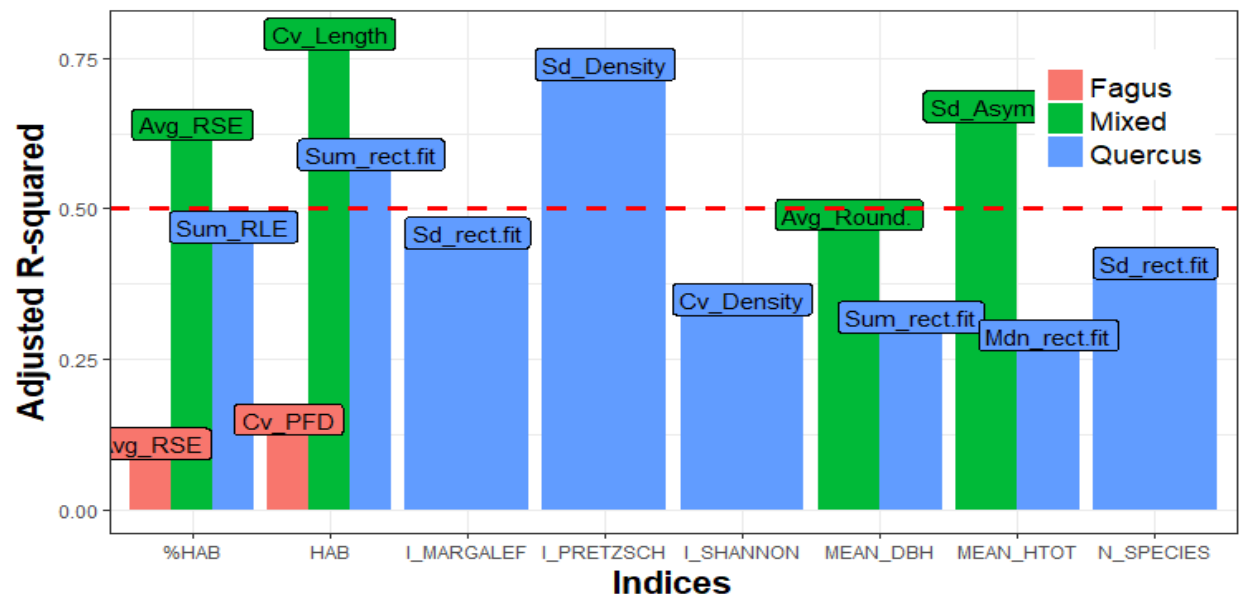
Fig2. Summary bar chart of adjusted R² from linear regression with living trees data in all the three forest types. On top of each bar the gap patch metric used for the linear regression

The study showed that in the examined forest types, all characterized by a stand exclusion development stage, horizontal structure, vertical structure and functional diversity of the forest can be assessed through forest canopy gaps. Of the many gap patch metrics, the shape metrics yielded best results compared to the extent ones such as the area of the gap. Therefore, the study suggests that a particular attention should be given to gap shapes as much as to gap sizes, when creating new gaps by silvicultural interventions.

Chapter 1. INTRODUCTION

1.1. Research problem

Reliable estimation of forest canopy attributes is important for many applications ranging from hydrology, carbon and nutrient cycling, and global change to forest management (Chianucci et al. 2016). In managed forests, namely, one of the most important tasks of foresters is the management of competition between trees, through selective thinning or opening of canopy gaps, to change the growing space of selected target trees and increase their growth. In addition, empirical studies have demonstrated that tree thinning, trees death and resultant changes in canopy gap structure impact forest regeneration and biodiversity of the understorey plants (Liu et al. 2011; Busing 1994; Popma and Bongers 1988; Barden 1981; Brokaw 1982; Boyd et al. 2013). Classically, sustainable forest management (SFM) indicators, defined as the basic tools for defining and promoting sustainable forest management (ForestEurope 2016), are obtained through repeated ground forest inventories (Corona et al. 2011).

Although this approach provides many benefits such as statistical reliability and high accuracy, it is expensive, time consuming and not flexible (Corona 2010). Hence, forest information can be hardly updated. Remotely sensed data is one of the best ways to monitor forest since the method is nondestructive and achievable even in inaccessible areas.

Airborne and satellite remote sensing has been used for long time in forestry for monitoring change in forest cover (Hansen et al. 2013; Nijland et al. 2015), estimating canopy height (J. Zhang, Nielsen, et al. 2016; Nijland et al. 2015), measuring tree density (Crowther et al. 2015); but it failed to provide the flexibility and the fine spatial resolution usually required in forest management and forest ecosystem monitoring (Getzin, Wiegand, and Schöning 2012; Anderson and Gaston 2013). This is particularly needed under the climate change scenarios predicting extreme events in Europe that will require a regular monitoring of forest ecosystems (Lehmann et al. 2015). Even though the stand-level information is critical for sustainable forest management (H. Zhang and Jim 2013), its extraction from medium to coarse spatial resolution images is a challenge (Tang and Shao 2015).

The technological advancement made available remote sensing by unmanned aerial vehicles (UAVs) or commonly known as drones which combine both the flexibility of data acquisition with a fine spatial resolution and a low cost (J. Zhang, Hu, et al. 2016; Näsi et al. 2015; Paneque-Gálvez et al. 2014; Zarco-Tejada et al. 2014; Wallace et al. 2016; Lehmann et al. 2015; Garcia-Ruiz et al. 2013; Colomina and Molina 2014; Dandois and Ellis 2013; Zahawi et al. 2015). UAVs offer as well the advantage of flying at low altitudes below the clouds (Meng et al. 2017; Lehmann et al. 2015; Lisein et al. 2015; Suárez et al. 2005; Bunting and Lucas 2006; Puliti et al. 2015). This allows very high spatial resolution images to be generated, with the potential to e.g. detecting forest infestation and damages at tree level (Lehmann et al. 2015; Hall et al. 2016; Michez et al. 2016; Myers, Ross, and Liu 2015). Notwithstanding all these advantages, the UAV's technology is relatively new in the scientific research compared to military applications (Lisein, Linchant, et al. 2013; Colomina and Molina 2014; Sandbrook 2015; J. Zhang, Hu, et al. 2016; Anderson and Gaston 2013; Puliti et al. 2015; Paneque-Gálvez et al. 2014; Turner, Lucieer, and Watson 2012).

The techniques and packages developed for the airborne and satellite images hardly suit UAV imagery and data because of different acquisition parameters (Turner, Lucieer, and Wallace 2014; Czapski et al. 2015). Furthermore, mapping some forest features such as forest canopy gaps, forest microhabitats, biodiversity presents a great challenge. Although some studies tried to overcome some of the challenges (Getzin, Wiegand, and Schöning 2012; Getzin, Nuske, and Wiegand 2014; Chianucci et al. 2016), they used methods rarely available at low cost or available as handy techniques for forest managers. The use of lightweight UAV can help exploring how canopy gaps affect forest regeneration or biodiversity of the forest understorey at low cost with not too sophisticated techniques.

1.2. General objective

The aim of this research is to assess at what extent forest features, from a small test site (240 ha) covered by deciduous forest dominated by beech and turkey oak in central Italy, could be extracted from UAV images by using forest canopy gaps as a proxy in order to supplement forest inventory data and achieve a sustainable forest management.

1.3. Specific objectives

i) Gap mapping
ii) Exploring correlations between gaps metrics and ground measured forest attributes,
iii) Modeling correlation by linear regression,
iv) Spatial estimation (or mapping) of selected forest attributes (those with the best fit of the regression model).

1.4. Hypotheses

- Forest canopy gaps (FCG) could be accurately mapped from UAVs' data
- Understorey data (biodiversity indices and structural composition) are correlated to FCG
- Living trees parameters are correlated to FCG
- Deadwood volume and composition is correlated to FCG
- Forest structural attributes can be predicted from FCG metrics

1.5. Thesis structure

1. This document is structured in five parts. After the introductory chapter, Chapter 2 deals with the state of art in the field of UAV as a platform and its remote sensing application in forestry,
2. Chapter 3 presents the study area, materials used in order to achieve the objectives, and finally methods,
3. Chapter 4 highlights the main findings and,
4. Chapter 5 gives a discussion of the main findings and their implication in forest management and inventories.

Chapter 2. LITERATURE REVIEW

2.1. Drones as a platform

The distinction between different types of drones is based on their weight and their size as well as their power, which limits their payload carrying capacity, operating altitude, and range (Anderson and Gaston 2013; Tang and Shao 2015). For example, Watts et al. (2012) classify drones into seven different categories while Anderson & Gaston (2013) classify them into four size classes: large, medium, small and mini, and micro and nano. Depending on the takeoff and the landing techniques, Tang & Shao (2015) distinguish two type of drones: horizontal takeoff and landing and vertical takeoff and landing. The characteristic of fixed-wing drones is the horizontal takeoff, whereas the rotary-wing drones perform a vertical takeoff. The fixed wing drones such as eBee (Anonymous 2017) are preferred when the coverage is large and the operator has minimal experience (Tang and Shao 2015). UAVs can carry different active or passive sensors such as multispectral cameras – operating in the visible, the near infrared (NIR), the short wave infra-red (SWIR), the thermal infrared (TIR) – radar and Lidar (Zarco-Tejada et al. 2014; Colomina and Molina 2014; Tang and Shao 2015).

The low operational flying altitude of unmanned aerial vehicles, usually in the range of 50–300 m, permits the acquisition of extremely high spatial-resolution imagery, with a resolution up to 1 cm/pixel (J. Zhang, Hu, et al. 2016; Del Pozo et al. 2014; Turner et al. 2014). This also generates a lot of aerial images. For instance, the coverage of 2 ha can yield around 150–200 images (Turner, Lucieer, and Watson 2012). In addition, UAVs have a very short time of flight (Whitehead and Hugenholtz 2014; Paneque-Gálvez et al. 2014). Moreover, there is a difference between images acquired by traditional aircrafts and the UAVs. The latter has high perspective distortion due to low altitude of the platform, a large rotational and angular variations between images, exterior orientation (EO) parameters are either unknown or, if measured, they are likely to be inaccurate (Y. Zhang, Xiong, and Hao 2011; Turner, Lucieer, and Watson 2012; Puliti et al. 2015).

Furthermore, images from UAVs denote a high variability in illumination (Turner, Lucieer, and Watson 2012; Drauschke, Bartelsen, and Reidelstürz 2014) and the ground resolution of the images differs from the one of tree tops (Drauschke, Bartelsen, and Reidelstürz 2014). Consequently, the use of UAVs for monitoring large forest stands can be regarded feasible only for small scale forestry applications. UAVs remote sensing presents specific challenges such as the elaboration of the mosaic image, the georeferencing and the generation of 3D cloud points through a process known as Structure from Motion (SfM).

Upon the collection of image strips, they are usually combined in a wide image covering the study area. This new composite image is known as a mosaic (Hung, Xu, and Sukkarieh 2014; Turner, Lucieer, and Watson 2012; X. Li and Shao 2014; Flynn and Chapra 2014; Näsi et al. 2016; Lisein et al. 2015). In practice, the algorithm used tries to align the strips of images by selecting a myriad of tie points from one each individual image and comparing them to all other images (Lehmann et al. 2015). Turner, Lucieer, and Watson (2012), Harwin and Lucieer (2012) assert that the most robust algorithm for creating UAV image mosaics is the Scale Invariant Feature Transform (SIFT) algorithm. In fact, SIFT is a region rather than a point detector. This leads to the availability of redundant information and therefore improving

the quality of the mosaicking. Once the mosaic image is obtained, it needs to be georeferenced.

The lightweight UAVs (see J. Zhang, Hu, et al. 2016a; Zahawi et al. 2015; Suomalainen et al. 2014) used in forestry applications do not possess onboard GPS/IMU of good quality (Turner, Lucieer, and Watson 2012) that could allow direct georeferencing (Turner, Lucieer, and Wallace 2014). Instead, ground control points (GCP) distributed in the image are used (Turner, Lucieer, and Watson 2012; J. Zhang, Hu, et al. 2016; Dandois and Ellis 2013; Wallace et al. 2016; Lehmann et al. 2015; Lisein et al. 2015; Turner et al. 2014) a process known as "indirect georeferencing" (Lisein, Linchant, et al. 2013). The two different methods can yield disparate results. The quality of the GPS/IMU used onboard determine the accuracy of direct georeferencing (Turner, Lucieer, and Wallace 2014) while the quality of the georeferencing using GCPs depends mainly on the possibility to discriminate these markers from the aerial image. In a study conducted in the Antarctic, Turner et al. (2014), demonstrated that the size of GCPs matters to locate GCPs on the aerial images as well as the spatial resolution of the images in the accuracy of georectification using GCPs. Furthermore, the GCPs georeferencing may underperform if the site is not accessible (Lehmann et al. 2015; Wallace et al. 2016) or if are not available open areas (e.g., clear-cuts, canopy gaps, agricultural fields) to install GCPs. Consequently, the georeferencing accuracy affects the compatibility of UAVs data to the ground-collected data. Nevertheless, Turner, Lucieer, and Watson (2012) in a comparative study found that the GCPs georeferencing had an accuracy of 10-15 cm, whereas the direct georeferencing performed poorly with an accuracy of 65-120 cm. Expanding on the same idea, Lehmann et al. (2015) assert that currently, the majority of micro UAV possess a GPS with accuracy ranging from 2 m to 13 m which is too inaccurate for direct georeferencing.

The third step usually performed is the generation of three-dimensional (3D) point clouds. Due to the fact that UAV images possess both the characteristics of the terrestrial images and aerial images (Turner, Lucieer, and Watson 2012), the SfM algorithm developed for computer vision can be utilized in UAV imagery to generate 3D photogrammetric point clouds. The 3D points are a suitable way of storing complex data (Harwin and Lucieer 2012). This data structure has been used in many studies to extract forest biophysical properties (e.g. Wallace et al. 2016; Lisein et al. 2013; Näsi et al. 2015; Dandois and Ellis 2013; Zarco-Tejada et al. 2014; Turner et al. 2014; Díaz-Varela et al. 2015; Puliti et al. 2015; Kachamba et al. 2016; Salamí, Barrado, and Pastor 2014).

It is important to notice that Turner, Lucieer, and Watson (2012) describe a different workflow for processing UAV imagery. In this workflow, the SfM algorithm is used to generate 3D cloud points which are then georeferenced. The 3D cloud points are later used to produce a digital terrain model (DTM) required for the rectification of images (producing hence ortho-images). And finally, the ortho-images are joined together to produce a mosaic known as ortho-mosaic.

With the intent to overcome the aforementioned problems of UAV images, Drauschke, Bartelsen, and Reidelstürz (2014) developed a method of using UAV imagery without elaborating an ortho-mosaic. Instead, the authors used original images. They argue the process suppress the need to balance the intensity value in the scene and to have a

constant image scale. The *sine qua non* condition for the success of the method is to possess images with sufficient matching points.

2.2. UAV's applications and data analysis

Since optical UAVs collect data with a very high spatial resolution, the treatment of these data differs from the analysis of the traditional airborne or aerial remote sensed data. The research for extracting forest attributes from UAVs data is a current topic. Some of the extracted attributes are on the stand level while others are limited to tree level while few go up to the landscape level.

Tree species composition of forest stands can be assessed by optical remote sensing. High-resolution imagery can help detecting the dominant forest canopy tree species, whereas foresters usually refer to species composition as the relative proportion of the number of stems per species regardless of its dominance (Fassnacht et al. 2016). This simple difference in the definition can lead to different interpretation of species composition. However, many authors have managed to map species composition using UAVs data. Hence, Ørka and Dalponte (2013), by combining the airborne laser scanning (ALS) data to optical images estimated both the crown species composition and the basal area species composition. Furthermore, they found that the estimation was more accurate in the coniferous forest compared to deciduous forest due to the low canopy closure in the former. Similarly, K. Zhang and Hu (2012), using data of 6 cm of ground sampling distance (GSD) classified urban trees. This classification was moreover improved from less than 75% to 86.1% when they incorporated textural features.

The forest canopy gaps constitute another important feature influencing biodiversity and natural regeneration capability (Getzin, Wiegand, and Schöning 2012; Getzin, Nuske, and Wiegand 2014; Yang et al. 2015). According to Muscolo et al. (2014), gaps increase the habitat diversity, fauna and flora diversity, and structural complexity. Although remote sensing is the best way to map forest canopy gaps (Getzin, Nuske, and Wiegand 2014), small forest gaps cannot be mapped using satellite remote sensing (Tang and Shao 2015). The solution nowadays relies on LiDAR and UAV imagery. However, the definition of canopy gap itself remains unclear and inconsistent in the literature (Zielewska-Büttner, Adler, Ehmann, et al. 2016b; Betts, Brown, and Stewart 2005). In addition, there is no clear shape and size of forest canopy gap (Seidel, Ammer, and Puettmann 2015) although it is known that gap shape and dimension considerably influence gap microclimate (Muscolo et al. 2014; Seidel, Ammer, and Puettmann 2015). In their study, Bonnet et al. (2015) defined canopy gaps as 'openings in the canopy with a minimum area of 50 m^2, a minimum width of 2 m and a maximum vegetation height of 3 m'. Getzin, Wiegand, and Schöning (2012) adopting a different definition, achieved to map canopy gaps of the size of 1 m^2 from a true colors UAV image of 7 cm spatial resolution, in beech dominated deciduous and mixed deciduous-coniferous forests in Germany. Furthermore, Getzin, Nuske, and Wiegand (2014) extracted forest gaps and their spatial pattern from ten different plots of 1 ha. The gap's mapping was validated using LiDAR data. The authors recommend collecting aerial data in a cloudy condition in order to reduce the effect of the shadow that could lead to dark pixels' misinterpretation as gaps. Finally, the gap age is an important aspect since it is correlated to the gap size due to the fact that gaps fill with time and the biodiversity is disparate between a newly opened gap and an old one (Muscolo et al. 2014). In addition, according to Muscolo et al. (2017),

canopy gap age and size are the primary factors affecting the regeneration besides the suitable substrate.

In the quest to map forest attributes at a low cost, Wallace et al. (2016) performed a comparative study on a small plot with variable trees' density using, on the one hand, 3D cloud data generated from RGB UAV imagery, and on the other hand, UAV based Lidar (or Laser Scanning, LS). They estimated the canopy cover and the CHM. They concluded that the 3D cloud points are capable of capturing structural information in the sparse forest but when the density and the forest structure become complex, LS should be favored. Likewise, Jensen and Mathews (2016) conducted a similar study. The two authors compared the capability of 3D points clouds from SfM and UAV LiDAR data to map the canopy height. The density of SfM 3D points was 198 points.m^{-2} while the LS was captured with 1.4 m linear spacing. The two datasets yielded similar results with R^2 around 90%.

One of the many forest attributes researchers focus on is the detection individual tree species from UAV's data. Lisein et al. (2015), for instance, studied the best time period and spectral images that could lead to a better discrimination of five deciduous tree species in a mixed deciduous forest. They strongly argued that the phenology state that optimized the classification result is the one that minimizes the spectral variation within tree species groups and, at the same time, maximizes the phenologic differences between species. The disparity in forest tree phenology is at the maximum during early spring and late autumn. The end of leaf flushing was the most efficient single-date time window that allows tree species discrimination. They acknowledged, however, that the use of multi-temporal data improved tree species discrimination although the optimal single time window led only to an error of 16%. Comparing the RGB to the CIR data, the authors affirmed that the former outperformed the latter. Furthermore, the gain in the combination of RGB and CIR data accounts only 4% over the use of only RGB data. Similarly, in order to delineate individual tree species, Näsi et al. (2016) used two cameras sensitive in the range 400 to 1600 nm wavelength to collect hyperspectral data with GSD ranging from 3 cm to 20 cm. They observed that not all the spectral range was necessary to discriminate the tree species under investigation. Although they managed to classify the five different species in the study area, they did not produce any accuracy evaluation on the approach.

Some researchers worked on the use of UAVs in riparian forests. Michez et al. (2016) detected from a 10 cm GSD RGB and CIR images some species composition and their health status in Belgium. Similarly, Husson, Ecke, and Reese (2016) used RGB images of 5 cm GSD to map aquatic vegetation in a 'Natura 2000' reserve in Sweden. They compared the automatic mapping to the manual one and summarized that the manual mapping of the non-submerged vegetation was possible although very time-consuming. Furthermore, comparing the threshold classification to the random forest (RF) classification, they found that the RF performed relatively poorly.

Other common tree stand parameters assessed by UAV remote sensing are: the coverage or density or Leaf Area Index (LAI) (Chianucci et al. 2016; Bustamante 2015), health status of the forest (Lehmann et al. 2015; Garcia-Ruiz et al. 2013; Näsi et al. 2015), the canopy height (Dandois and Ellis 2013; Zarco-Tejada et al. 2014; Lisein, Pierrot-Deseilligny, et al. 2013) and mapping of forest community (Bunting et al. 2010) . The tree level parameters usually studied from UAV's sensed data are: the tree height using LiDAR data (Wallace et al. 2016;

Dandois and Ellis 2013; Zhen, Quackenbush, and Zhang 2016) and individual tree crown width (Díaz-Varela et al. 2015; Zhen, Quackenbush, and Zhang 2016; Bunting et al. 2010; Meng et al. 2017). A more detailed list of studies using UAV data to map forest attributes is given in Table 2-1.

Depending on different forest attributes under investigation, various methods are used. Methods themselves vary according to data collected (spatial and spectral resolution of images). However, regardless of the data, the first analysis most of the authors working on very high-resolution images from UAVs perform is the segmentation in order to achieve an object-based image analysis (OBIA) which is based on the classification of objects (for example: individual tree crown) rather than pixels (X. Li and Shao 2014; Bunting and Lucas 2006; M. Li et al. 2016; Singh et al. 2015; Moskal, Styers, and Halabisky 2011; Puissant, Rougier, and Stumpf 2014; Lehmann et al. 2015).

Individual tree crown detection is important because it allows quantifying vegetation density, to monitor the vegetation change and finally the classification of tree species (Hung, Bryson, and Sukkarieh 2012). The first step in identifying individual tree crown condition is the delineation of the individual crown itself. Delineation of tree crown has been under investigation since the 1990s (Erikson 2004). Hence, a number of methods have been developed with each one underlying on a specific theory. Hung et al. (2012) described the valley growing and the region growing algorithms. These two algorithms though very common in computer vision field, perform poorly in detecting tree crowns since in forests tree crown edges are not sharp (Hung, Bryson, and Sukkarieh 2012).

The most common segmentation algorithm in forestry is multi-resolution (MR) segmentation and it reveals effective in separating an image into meaningful image objects even though it presents a drawback of being very slow (X. Li and Shao 2014). The other two common algorithms are the multi-threshold (MT) segmentation and quadtree-based (QT) segmentation. The latter represents images at multiple resolutions based on the pixel values within a given image object: the absolute difference of pixel values within the image object is compared with a threshold value (a user defined scale parameter). MT segmentation splits an image object domain according to the pixel value(s) assigned to the thresholds (X. Li and Shao 2014). To successfully perform the segmentation, many authors supplement the spectral data with some vegetation indices (Candiago et al. 2015; Rasmussen et al. 2016; Garcia-Ruiz et al. 2013; Quiros and Khot 2016) and textural features (Feng, Liu, and Gong 2015; Moskal, Styers, and Halabisky 2011).

Table 2-1. Summary of studies mapping forest attributes from UAV data

Sensor camera…	Resolution	Target variable	Data processing	Accuracy (where appropriate)	References
LiDAR	40 points/m²	-Canopy gap -CHM	Image segmentation Pixel classification Raster threshold	K=0.82	(Bonnet et al. 2015)
	100-1500 points/m²	-Ind. Height -CHM -DBH	Segmentation	SD= 34 cm RMSE = 2.1 cm	(Jaakkola et al. 2010)
	7.2 points/m²	-Species composition	individual tree crown (ITC) approach; semi-individual tree crown (SITC) approach; and area-based approach (ABA).	K=0.56 to 0.91 RMSE= 0.25 to 3.5 cm	(Ørka and Dalponte 2013)
	13 points/m²	-HDom -Ind. height	Linear regression	R^2= .86 RMSE=1.45m R^2= .94 RMSE=.83m	(Lisein, Pierrot-Deseilligny, et al. 2013)
	174 points/m²	-Canopy cover -Tree height	Linear regression	RMSE= 0.92m	(Wallace et al. 2016)
	50 points/m²	-Tree height -Crown area -Crown volume -CHM	α-shape algorithm	RMSE=0.4 to -0.7 RMSE = 4.61 m² - MD< 0.35 m	(Wallace, Musk, and Lucieer 2014)
	145 - 220 points/m²	-CBH -Pruning detection	-	RMSE=0.60 m Rate of detection 96% to 125%	(Wallace, Watson, and Lucieer 2014)
	8-62 points/m²	-Tree height -Crown width	-	Sd= 0.15 m to 0.26 m Sd= 0.69 m to 0.61 m	(Wallace et al. 2012)
	1.4 points/m	-CHM	Linear regression	R^2= 0.89 to 0.90	(Jensen and Mathews 2016)
RGB camera	7 cm	-Gap size	-Manual segmentation -Regression	R^2=0.74	(Getzin, Wiegand, and Schöning 2012)
	7 cm	-Gap size -Gap pattern	Manual delineation Statistical analysis	-	(Getzin, Nuske, and Wiegand 2014)
	6.8–21.8 cm	-Vegetation units -standing dead wood	Pixel-based analysis Segmentation (OBIA)	K=0.79 Omission (80%) and commission (65%) errors	(Dunford et al. 2009)
	7.5 cm	-LAI -Canopy cover -Gaps between crowns	GLA LAB2 classification	R^2=0.59 to 0.70	(Chianucci et al. 2016)
	13 cm	-Canopy gap	Segmentation Textural analysis	R= 0.30 to 0.43	(Nyamgeroh 2015)
	20 cm	-Species	Segmentation Random Forest	OOB = 16%	(Lisein et al. 2015)
	5 cm	-Species -Growth form	Segmentation RF Threshold	Accuracy 52% to 99%	(Husson, Ecke, and Reese 2016)
	1.37 – 5.31 cm	- understorey invasive plant	winSCANOPY	Accuracy 0% to 100%	(Perroy, Sullivan, and Stephenson 2017)
	7.6 cm	-HDom -Ind. height	Linear regression	R^2 = .82 RMSE=1.65m R^2 = .91 RMSE=1.04m	(Lisein, Pierrot-Deseilligny, et al. 2013)
	2 cm	-Pest infestation -Canopy gaps	Segmentation	K=0.78 to 0.82	(Lehmann et al. 2015)

Sensor camera...	Resolution	Target variable	Data processing	Accuracy (where appropriate)	References
VIS/NIR camera	15 cm	-Defoliation	Supervised classification	-	(Castedo-Dorado et al. 2016)
	10 cm	-species -health status	Multiresolution segmentation Random forest	Accuracy of 79.5 % to 84.1 % Accuracy of 81.% to 90.6%	(Michez et al. 2016)
	10 cm	-Stem volume -Species identification	-	-	(Salo et al. 2012)
	10 cm	-Species identification	Supervised classification Unsupervised classification	Accuracy of 50% to 80%	(Gini et al. 2014)
3D point clouds	55 points/m^2	-Canopy height -AGB -Canopy openness -Canopy roughness	Ecosynth	$R^2>0.85$ $R^2>0.81$ $R^2>0.82$ $R^2>0.53$	(Zahawi et al. 2015)
	30–67 points/m^2	-CHM -CHP -AGB	Linear regression Ecosynth	$R^2= 0.63$ to 0.84	(Dandois and Ellis 2013)
	1-5652 points/m^2	-Canopy cover -Tree height	Linear regression	RMSE= 1.3m	(Wallace et al. 2016)
	500–700 points/m^2	-Ind. Tree detection -species identification	Local maxima Classification	Accuracy = 40% to 95% F-Score= 0.85 to 0.93	(Nevalainen et al. 2017)
	198 points/m^2	-CHM	Linear regression	$R^2= 0.89$ to 0.91	(Jensen and Mathews 2016)
	-	-Stems identification	3D reconstruction	$\rho= 0.696.$	(Fritz, Kattenborn, and Koch 2013)
	-	-Biomass	Multiple regression	RMSE = 46.7%	(Kachamba et al. 2016)
	-	- h_L - HDom -Stem number -Basal area -Stem volume	Linear regressions	R^2 0.71 RMSE= 13.3% R^2 0.97 RMSE= 3.5% R^2 0.60 RMSE= 39.2% R^2 0.60 RMSE= 15.4% R^2 0.85 RMSE= 14.5%	(Puliti et al. 2015)
	278 points/m^2	-CHM	Linear regression	RMSE=42 cm	(Lin, Lo, and Huang 2016)
	1890 points/m^2 10385 points/m^2	-Diameter -Height	Combination of aerial and terrestrial images	RMSE<1 cm RMSE=1 m	(Mikita, Janata, and Surový 2016)
	3406-5124 points/m^2	-CHM -Ind. tree delineation	Filter and local maximum algorithm	R^2 0.64–0.81 R^2 0.46–0.64	(D. Li et al. 2016)
	6.2–7.7 cm point spacing	-Top-of-canopy height -Aboveground carbon density	Correlation	R^2 0.86 RMSE= 2.5 R^2 0.85 RMSE= 3.9	(Messinger, Asner, and Silman 2016)

CHP = canopy height profile, MD=Mean absolute Deviation, CBH= Canopy Base Height; h_L= Lorey's mean height; k=Kappa index,

To successfully perform the OBIA classification, researchers working on UAV's data possess a large number of statistical and machine learning classification algorithms such as Linear Discriminant Analysis (LDA) (Garcia-Ruiz et al. 2013; M. Li et al. 2016; Roth et al. 2015), Random Forest (RF) (Puissant, Rougier, and Stumpf 2014; Belgiu and Drăgu 2016; Feng, Liu, and Gong 2015; Stumpf and Kerle 2011; M. Li et al. 2016; Lisein et al. 2015; Nevalainen et al. 2017; Michez et al. 2016; Drauschke, Bartelsen, and Reidelstürz 2014), K-Nearest Neighbor (KNN) (M. Li et al. 2016; J. Zhang, Hu, et al. 2016; Lehmann et al. 2015; Nevalainen et al. 2017), and Support Vector Machines (SVM) (Garcia-Ruiz et al. 2013; M. Li et al. 2016; Pelletier et al. 2016; Puissant, Rougier, and Stumpf 2014). Although classification algorithms are diverse, they do not have the same performance. M. Li et al. (2016) suggest that the SVM and RF are the best algorithms for classification and whenever possible, RF should be favored over the SVM. The RF classification is computationally efficient and not sensitive to the over fitting (Belgiu and Drăgu 2016; Puissant, Rougier, and Stumpf 2014). Nevertheless, Ma et al. (2015) acknowledge that many segmentation factors, including scales, features, samples and mixed objects can influence the classification algorithm performance.

Chapter 3. MATERIALS AND METHODS

3.1. Study area

The test site is located in Monte Venere, which is part of the natural reserve "Riserva Naturale del Lago di Vico". The natural reserve has been established by the Lazio Region Law No. 47 of 28.10.1982. Its territory comprises some of 4110 ha, in the municipalities of Caprarola and Ronciglione (Province of Viterbo, Lazio Region).

The landscape of the Natural Reserve is mostly flat around the lake of Vico but includes also several reliefs such as M. Fogliano (965 m), Poggio Nibbio (896 m), Poggio Gallesano (839 m) and Monte Venere (835 m). Mean annual rainfall ranges between 800 and 850 mm per year.

Forest areas cover about 750 in the Natural Reserve. Forest cover is characterized by deciduous high forests dominated by beech, turkey oak and mixtures of the two species.

The Natural Reserve includes also two Sites of Community Importance (SCI) called "Monte Fogliano and Monte Venere" and "Lago di Vico" and a Special Protection Area (SPA) "Lago di Vico - Monte Fogliano and Monte Venere".

The test site covers about 240 hectares within the larger area of the SCI "Monte Fogliano and Mount Venere"(618 hectares). The beech forest areas protected by the SCI are reported as priority habitats of Community interest (the Apennines beech forests with *Taxus* and/or *Ilex*).
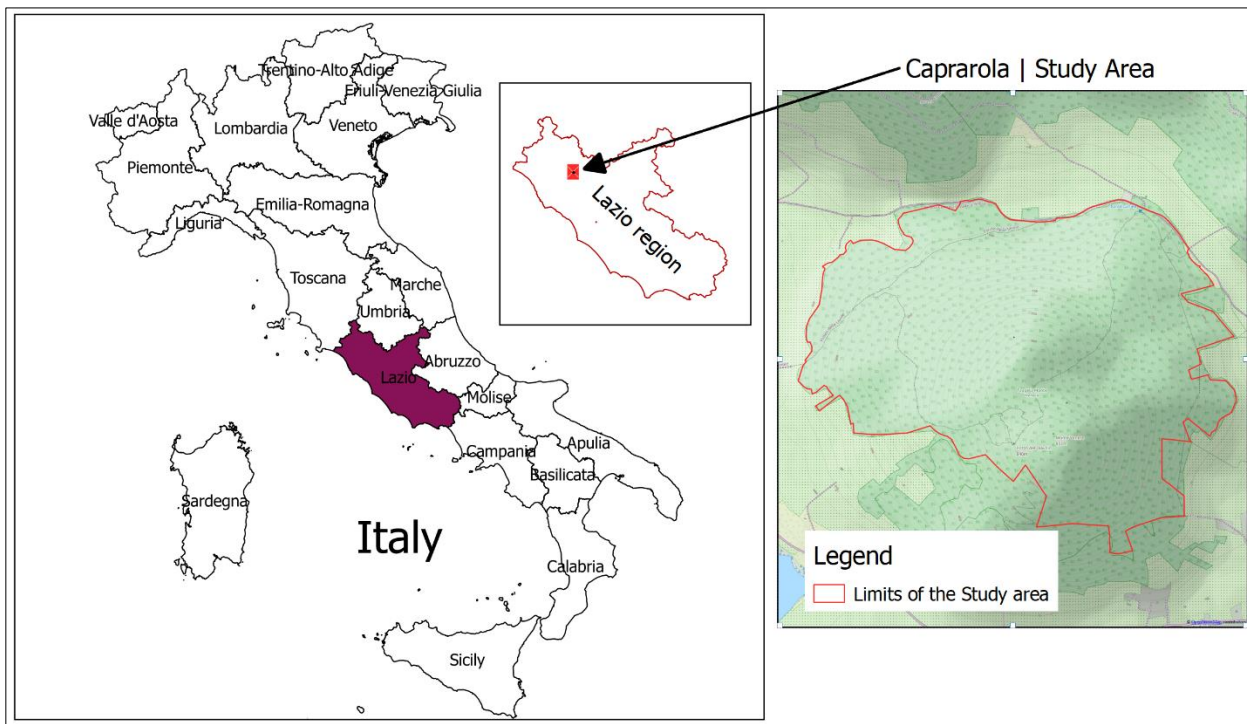
Figure 3-1. Location of the Study area (background: Openstreet Landscape map)

The presence of very fertile volcanic soils and the particular microclimate, related to the presence of the lake, create favorable conditions for the growth of beech, even at a low elevation. In fact, the conformation of the basin, the frequent formation of mists, the high relative air humidity and the protection from extreme winds ensure a suitable habitat for this species. As result, the beech forest of Monte Venere has a relevant ecological importance as it grows at much lower altitudes (around 500 m above sea level) than those usually occupied by beech in the Central Apennines (optimum between 1,000 and 1,700 m asl).

Beech forest of Monte Venere belongs to the *Aquifolio-Fagetum* association, that seems to reach the extreme northern boundary of its ecological range in the Province of Viterbo (Scoppola and Caporali 1998). Beech is usually accompanied by other deciduous trees like *Quercus cerris* L. (turkey oak) - in the upper layer and only at lower altitudes, *Carpinus betulus* L. (hornbeam*), Castanea sativa* Mill. (Chestnut), *Acer opalus* L. (maple), *Corylus avellana* L. (hazel), *Ilex aquifolium* L. (holly) - in the dominated in layer -.

Turkey oak becomes the dominant species in the reliefs facing south. Turkey oak forests also contain accompanying species such as ash (*Fraxinus ornus* L.) and hornbeam (*Ostrya carpinifolia* L.). Turkey oak forests present a well-developed shrub layer including *Rosa canina* L., *Cornus sanguinea* L., *Crataegus monogyna* Jacq., *Crataegus oxychanta* L., *Ruscus aculeatus* L.

All the forests in Monte Venere are in an early development stage, equivalent to the stand exclusion stage *sensu* Oliver and Larson (1996).

3.2. Field data collection

A field survey was performed in the framework of the FRESh LIFE project on fifty squared plots of 23 meters' side (area of the plot 529 m^2). In each plot, all plants (trees and shrubs) with a dbh > 2.5 cm were inventoried. The spatial position of the inventory plot (x, y coordinates of the center of the plot) was recorded with GNSS receivers with a sub-meter accuracy. Field data on tree and shrubs occurring in the field plots were used in the present study to assess species composition and diversity of the understorey layer and its relationships with gap features.

Data were collected on three different levels. Firstly, the understorey data. We followed along with Assmann (1970) defining the understorey as the layer representing 0-50% of the maximal height of the stand. For the understorey, and in each plot, we recorded the number of plants (trees) (N_PLANTS), the number of species (N_SPECIES), the Shannon index (H') (Shannon 1948), the Pielou index (I_PIELOU) (Pielou 1975), the mean DBH (MEAN_DBH), the average total height (MEAN_HTOT), the averages of total understorey volume (V_TOT) and basal area (G_TOT).

Secondly, we collected on living trees data such as the number of habitat trees (HAB), the percentage of habitat trees (%HAB) out of total plants in the plot, the mean DBH, the mean total height of the living trees in the plot, the index of Pretzsch (I_PRETSCH), the index of Shannon (I_SHANNON), the index of Margalef (I_MARGALEF) (Clifford and Stephenson 1975), the mean DBH, the mean total height. Bütler et al. (2013) define habitat trees are as standing live or dead trees providing ecological niches (microhabitats) such

as cavities, bark pockets, large dead branches, epiphytes, cracks, sap runs, or trunk rot. They are usually very large and old trees (Figure 3-2).
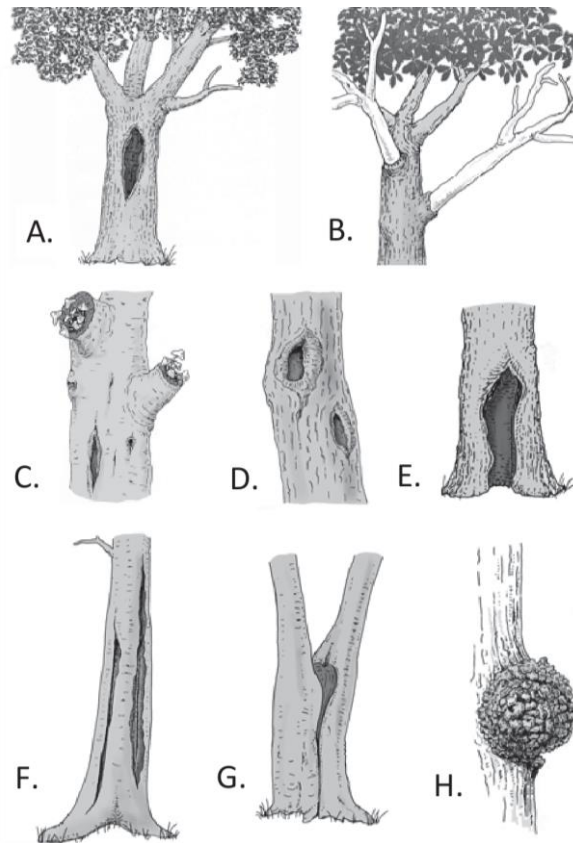
Figure 3-2. Different microhabitat types. A. Nonwoodpecker cavity, B. Canopy deadwood, C. Fruit-bodies of saproxylic fungi, D. Cavities with mould, E. Root-buttress cavity, F. Cracks, G. Fork split, H. Burr (Bütler et al. 2013)

Thirdly, in each plot, we recorded total volumes of lying deadwood (TOT_LYING), the standing dead wood (TOT_STAND) and stumps (TOT_STUMP). We distinguished as well, the total of dead wood in different decay classes (VOL1, VOL2, VOL3, VOL4, and VOL5), and the total volume of deadwood (VOL_TOT).

Table 3-1. Summary of diversity indices

Indices	Formulae	Range of variation	Description
Shannon index (H')	$-\sum p_i \ln(p_i)$	[0,ln(S)]	It expresses the frequency of the i-th species in a community, takes values generally between 0 and 3.5; higher values correspond to higher species diversity. Its maximum value (MAX_SHANNON) is given by the natural logarithm of the number of species found in the test area and occurs when all species are equally present.
Pielou index (E)	$H'/\ln(S)$	[0,1]	The index measures the relative abundance of species groups. The

			index can take values between 1 (all species are equally abundant) and 0 (there is only one species).
Pretzsch index (A_p)	$$-\sum_{i=1}^{S}\sum_{j=1}^{Z} p_{ji}\ln(p_{ij})$$	[0,ln(SxZ)]	The index summarizes and quantifies species diversity and the vertical distribution of species in a forest. The index is lowest in one-story pure forests, whereas it rises for pure forests with two or more stories. Peak values are reached in mixed woodlands with heterogeneous structures.
Margalef index (D)	$(S-1)\ln(N)$	[0,∞)	It quantifies the presence of a number of species in a community. It also depends on the number of plants found in the sampling area. The index grows with increasing species diversity.

S=number of species; *N*= total number of plants; *pij*= the frequency of specie *i* in the layer *j*; *pi*= frequency of the specie *i*. *z*= number of layers

3.3. UAV imagery collection

Aerial images covering the test site area were collected in May 2016 by the fixed-wing eBee drone (SenseFly, Cheseaux-Losanne, Switzerland, Figure 3-3), in the framework of the LIFE Project FRESh LIFE – Demonstrating Remote Sensing integration in sustainable forest management (https://freshlifeproject.net/). The eBee was equipped with a commercial 18.2 MP RGB camera. The eBee, a hand-launched and autonomous flying drone with an electric motor-driven pusher propeller, has a 96 cm wingspan and a weight of about 700 g including camera, inertial measuring unit, GPS and battery payloads. The maximum area covered in a single flight is about 12 km^2 in a maximum flight time of 45 min. By using the onboard navigation units, the horizontal/vertical accuracy ranges from 1 m to 5 m. The eBee flight plan was managed through SenseFly's eMotion software and the flight monitored through a laptop; the software requires an initial parameter like the area of interest, desired GSD, side and longitudinal image overlap. The software then automatically calculates the number of stripes to cover the area of interests and the flight height. Take-off and landing are also planned and managed by the software and monitored through the laptop. The controller has the ability to remotely control the UAV during the flight by the means of wireless modem connected to the laptop up to a distance of 3 km from the vehicle.

Figure 3-3. A view of the eBee drone (source: https://www.sensefly.com/drones/accessories.html)
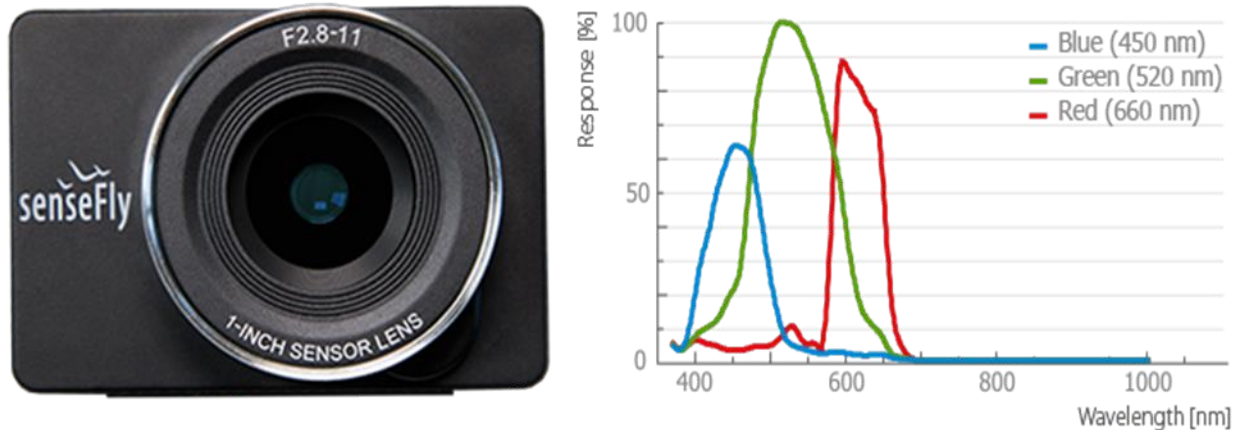
Figure 3-4. eBee RGB camera (left) and its spectral band responses (right) (source: www.sensefly.com/drones/accessories.html).

The eBee possesses two different sensors. The RGB sensor with sensibility in blue (450 nm), green (520 nm) and red (660 nm) (Figure 3-4). The second sensor, a 12MP camera, provides green (550 nm), red (625 nm) and the NIR (850 nm) band data (Figure 3-5).

Prior the takeoff, GCPs were placed and their coordinates were accurately measured.

Image strips were combined into a very high resolution RGB (10 cm pixel) and CIR (20 cm) orthomosaics. In order to map canopy gaps, the RGB orthomosaic was preferred, being characterized by a higher spatial resolution and higher tonal contrast compared to the CIR orthomosaic (Figure 3-6).
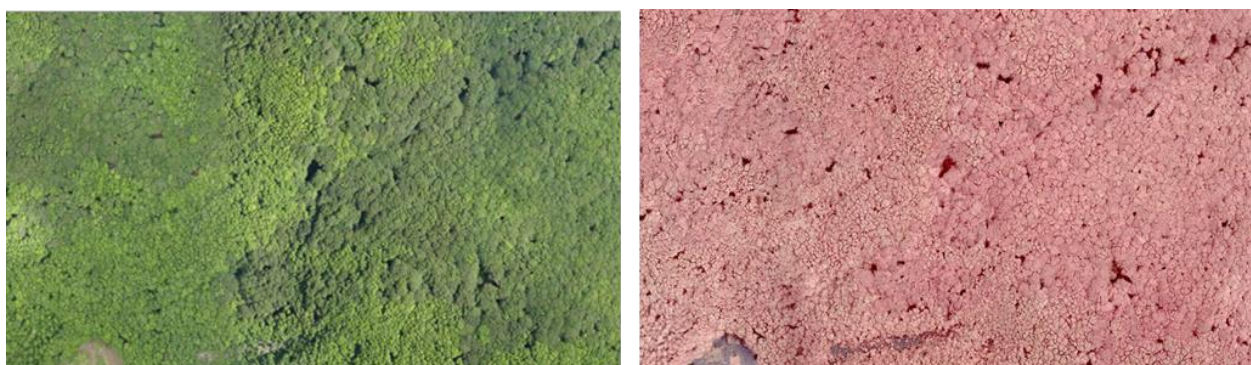
Figure 3-6. RGB true colors orthomosaic (left) and NIR false colors orthomosaic (right)

3.4. Image processing and variable selection

We tested different settings of the Contrast Split segmentation algorithm to map forest canopy gaps from the red band of the RGB orthomosaic. The red band was the only one significantly contrasting canopy gaps and crowns. The Contrast split algorithm is considered effective in separating objects of different contrasts, particularly dark objects from bright ones (Dezso et al. 2012). The idea of testing different settings is to extract as accurately as possible forest canopy gaps as well as intra-trees canopy gaps. This process was accomplished using eCognition Developer (http://www.ecognition.com) software. We validated the gap delineation by visual interpretation of the original orthomosaic. The visual validation techniques have been often used in forest canopy gaps mapping (Zielewska-Büttner, Adler, Ehmann, et al. 2016a). We later tested different thresholds to discriminate small gaps which might not affect ecological phenomena under investigation and therefore constitute a noise masking relevant data. We only considered gaps falling within the plot boundary and gaps within the plot boundary for at least 50% of their area. For each gap, we calculated the shape and size indices, and other gap patch metrics commonly used in landscape-scale analyses (Getzin, Wiegand, and Schöning 2012).

16

These gap patch metrics are the area (*A*), the length (l_v), the border length (or the perimeter, b_v), the ratio length/width , the width, border index (*B.Index*), asymmetry (*Asym*), roundness (*Round*), compactness (*Comp*), shape index, density, rectangular fit (*Rect.fit*), radius of the largest enclosed ellipse (*RLE*), radius of the smallest enclosed ellipse (*RSE*), elliptic fit and other composite indices such as the shape complexity index (*GSCI*). The gap shape complexity index is an important measure of forest gaps (Koukoulas and Blackburn 2004). It is the ratio of a gap's perimeter to the perimeter of a circular gap of the same area. A value of 1 describes a perfect circle while increasing values indicate increasing shape complexity. For example, values of 1.20 and 2.70 have 20% and 170% complexity, respectively. The last three gap metrics are the patch fractal dimension (*PFD*) (Moser et al. 2002), the fractal dimension (*FD*) (Eysenrode et al. 1998) and the fractal dimension index (*FDI*) (Saura and Carballal 2004). Thus, all 19 patch metrics (see Table 3-2 and for more explanation refer to eCognition Reference Book) emphasize different nuances of two- dimensional gap properties that may be potentially important for linking image-detected higher-level structures to dependent lower- level processes of the biota.

For each patch metric, we calculated the median (mdn), the mean (avg), the standard-deviation (sd), the sum (sum), and the coefficient of variation (cv). This leads to 95 variables for each plot. We tested gap metrics with two different area thresholds namely of size greater than 1 m^2 and greater than 2 m^2. These two thresholds are set because some ecological phenomena, such as understorey structure dependencies, are only quantifiable if small gaps are taken into account, yet very small gaps may not affect at all the lower dependency phenomenon, constituting, therefore, a noise (Busing 1994).

Table 3-2. Summary description of patch metrics

Patch metric	Formula	Value range	Description
Area (A)			
Border length (b_v)		$[0, \infty)$	Is basically the perimeter of the gap
Length (l_v)	$\sqrt{P_v \cdot \gamma_v}$	$[0, \infty)$	P_v is the total number of pixels contained in the patch v γ_v is the length-width ratio of an image object v
Length/Width (γ_v)	-	$[0, \infty)$	The length-to-width ratio of an image object
Width (w_v)	$\dfrac{P_v}{\gamma_v}$	$[0, \infty)$	The width of an image object is calculated using the length-to-width ratio
Asymmetry	-	$[0,1]$	The Asymmetry feature describes the relative length of an image object, compared to a regular polygon. An ellipse is approximated around a given image object, which can be expressed by the ratio of the lengths of its minor and the major axes. The feature value increases with this asymmetry.
Border Index	$\dfrac{b_v}{2 \cdot (l_v + w_v)}$	$[1, \infty)$ 1=ideal	The Border Index feature describes how jagged an image object is; the more jagged, the higher its border index. This feature is similar to the Shape Index feature, but the Border Index feature uses a rectangular approximation instead of a square.

17

Patch metric	Formula	Value range	Description
			The smallest rectangle enclosing the image object is created and the border index is calculated as the ratio between the border lengths of the image object and the smallest enclosing rectangle
Compactness	-	$[0, \infty)$ 1=ideal	The Compactness feature describes how compact an image object is. It is similar to Border Index, but is based on area. However, the more compact an image object is, the smaller its border appears. The compactness of an image object is the product of the length and the width, divided by the number of pixels.
Density	-	[0, depending on shape of image object]	The Density feature describes the distribution in space of the pixels of an image object. In eCognition Developer 9.0 the most "dense" shape is a square; the more an object is shaped like a filament, the lower its density. The density is calculated by the number of pixels forming the image object divided by its approximated radius, based on the covariance matrix
Elliptic Fit	-	$[0,1]$; 1 = complete fitting, 0 = <50% fit.	The Elliptic Fit feature describes how well an image object fits into an ellipse of similar size and proportions. While 0 indicates no fit, 1 indicates a perfect fit. The calculation is based on an ellipse with the same area as the selected image object. The proportions of the ellipse are equal to the length to the width of the image object. The area of the image object outside the ellipse is compared with the area inside the ellipse that is not filled by the image object
Radius of Largest Enclosed Ellipse (ε_v^{max})	-	$[0, \infty)$	The Radius of Largest Enclosed Ellipse feature describes how similar an image object is to an ellipse. The calculation uses an ellipse with the same area as the object and based on the covariance matrix. This ellipse is scaled down until it is totally enclosed by the image object. The ratio of the radius of this largest enclosed ellipse to the radius of the original ellipse is returned as a feature value.
Radius of Smallest Enclosing Ellipse (ε_v^{min})	-	$[0, \infty)$	The Radius of Smallest Enclosing Ellipse feature describes how much the shape of an image object is similar to an ellipse. The calculation is based on an ellipse with the same area as the image object and based on the covariance matrix. This ellipse is enlarged until it encloses the image object in total. The ratio of the radius of this smallest enclosing ellipse to the radius of the original ellipse is returned as a feature value.
Rectangular Fit	-	$[0,1]$; where 1 is a perfect rectangle.	The Rectangular Fit feature describes how well an image object fits into a rectangle of similar size and proportions. While 0 indicates no fit, 1 indicates for a complete fitting image object. The calculation is based on a rectangle with the same area as the image object. The proportions of the rectangle are equal to the proportions of the length to width of the image object. The area of the image object outside the rectangle is compared with the area inside the rectangle.
Roundness	$\varepsilon_v^{max} - \varepsilon_v^{min}$	$[0, \infty)$; 0 = ideal	The Roundness feature describes how similar an image object is to an ellipse. It is calculated by the difference of the enclosing ellipse and the enclosed ellipse.

Patch metric	Formula	Value range	Description
Shape Index	$b_v / 4\sqrt{A}$	$[1,\infty)$; 1 = ideal	The Shape index describes the smoothness of an image object border. The smoother the border of an image object is, the lower its shape index
Gap shape complexity index (GSCI)	$b_v / \sqrt{4\pi A}$	$[1,\infty)$; 1 = perfect circle	It is the ratio of a gap's perimeter to the perimeter of a circular gap of the same area
Patch fractal dimension (PFD)	$2 \bullet ln(b_v) / ln(A)$	-	-
Fractal dimension (FD)	$2 \bullet ln(b_v / 4) / ln(A)$	-	-
fractal dimension index (FDI)	$2 \bullet ln(b_v / \sqrt{4\pi}) / ln(A)$	-	-

3.5. Forest types maps

In the framework of the FRESh LIFE project the RGB orthomosaic was classified by visual image interpretation, a qualitative image classification technique widely applied by forest practioners for forest cover typing. The high spatial resolution of RGB orthomosaic is fine enough that by a combination of tone, size, shape and texture criteria individual trees can be identified to genus or species by their branching habit and spectral response. Differences in tone in the green band were the fundamental criterion for mapping the three main forest cover types occurring the study area: beech, turkey oak or mixed beech and turkey oak.

On the field, we determined three types of forest (turkey oak, beech, and mixed) identified on the basis of the percentage contribution of the basal area of the dominant species (beech and oak) within trees (Figure 3-7). The forest type has been defined as:

- Pure (beech or oak): where beech or oak contributes at least 85% to the total basal area determined for the stumps; or where none of the two species reach the 85% threshold and one of them contributes less than 15%. In the latter case, the forest type assigned to the plot is that of the main species that offers the greatest contribution;
- Mixed: when it is an intermediate situation
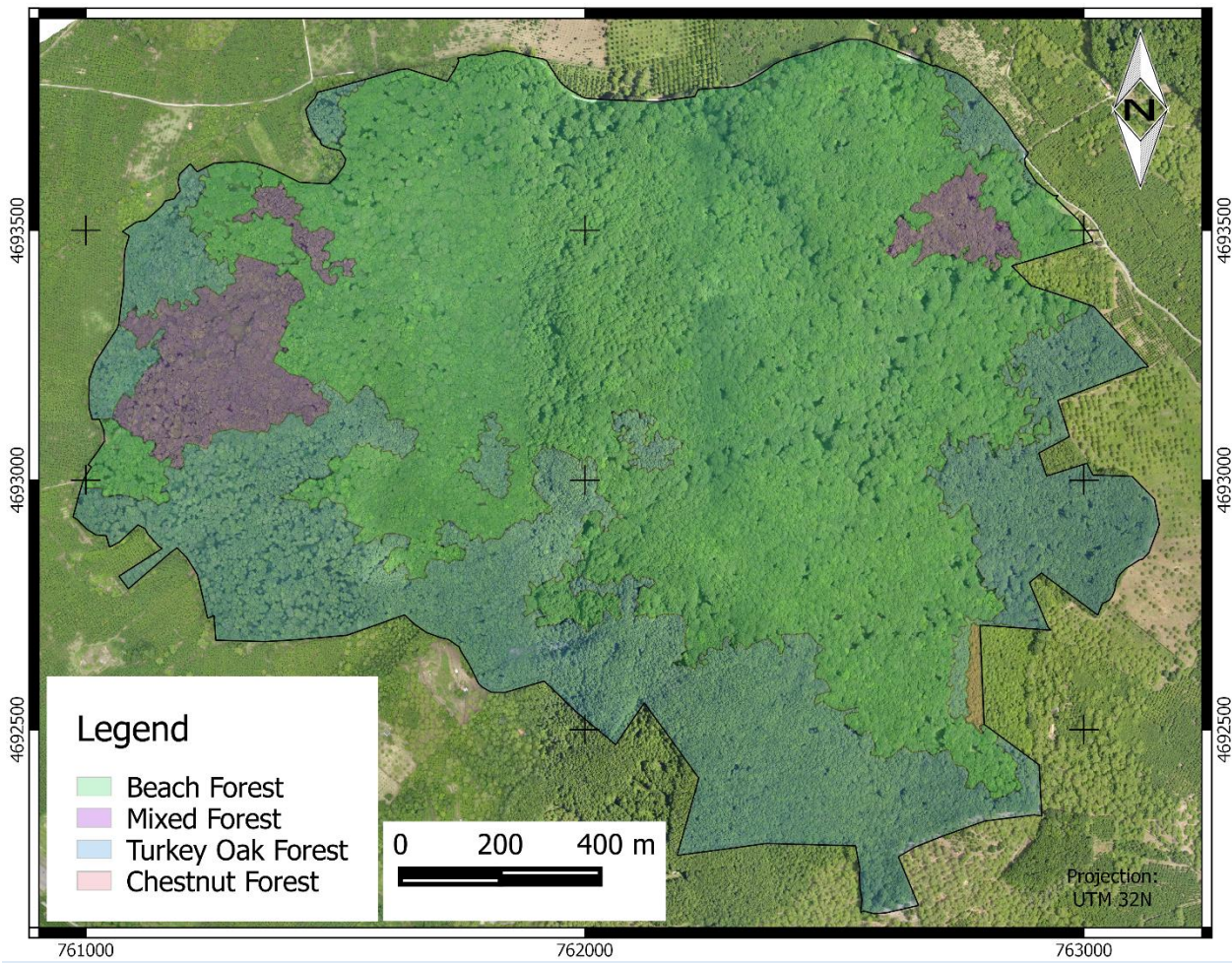
Figure 3-7. Map of forest types. eBee RGB imagery overlaid by type of forest according to European Forest Type Frame in the Caprarola forest

3.6. Statistical analyses

We applied several statistical analyses to test the dependence among image based variables called patch metrics and field data parameters. Firstly, we performed exploratory analysis on the data. Therefore, we performed the ANOVA (Analysis of Variance) when the distribution is normal or the KRUSKAL-WALLIS analysis otherwise with the categorical variable being the forest type characterizing each single plot (cf. § 3.5). This analysis allowed to determine whether the field parameter should be split into forest type for further analysis or could be taken as a whole.

We used all gap variables for Pearson's product-moment correlation analysis and Spearman's rank correlation with the field data. Usually, the two correlations give approximately the same results (see Main-Knorn et al. 2011). To avoid that the observed correlation, although significant according to the p-value lower than 5%, could have happened by chance, its significance was further thoroughly tested using the 9999 permutation method proposed by Legendre and Legendre (1983). Indeed, the authors assert: 'permutation provides an efficient approach to testing when the data do not conform to the distributional assumptions of the statistical method one wants to use (e.g. normality). Permutation testing is applicable to very small samples, like nonparametric tests.'

Therefore, permutation method perfectly fits our study. Furthermore, this method has been successfully used by some researchers investigating the relationship between forest canopy gap metrics and biodiversity (Getzin, Wiegand, and Schöning 2012).

For gap variables correlated with field data, we tested the correlation among significant potential predictors. This second step allowed to decrease the redundant information brought by correlated potential predictors and eliminate the collinearity or singularity. To determine the most significant variables to be used as possible predictors we used a forward stepwise analysis. The forward stepwise is known to select only the most significant predictors as opposed to the backward that eliminates the least significant ones. Therefore, the forward stepwise approach leads to a model with the minimal necessary number of variables only.

When the forward stepwise yielded only one predictor variable as sufficient to model the field parameter, we compared the correlation coefficients of Spearman and Pearson. If these two coefficients are significant and close to each other, then the patch metric is selected as a predictor. Otherwise, the variable denoting both Spearman and Pearson coefficients significantly high is selected as the most determinant. This approach has the advantage of; on the one hand excluding variables depicting high Pearson's correlation due to extreme values, and on the other one, not solely relying on the Spearman's correlation which is a measure of monotony (Hauke and Kossowski 2011) and not of linearity. We performed the correlation analysis using the *Hmisc* package (https://cran.r-project.org/web/packages/Hmisc/index.html).

Finally, we performed the linear regression using the selected significant variables. Following the lines of Møller and Jennions (2002) and Getzin, Wiegand, and Schöning (2012), who considered a coefficient of determination $R^2 > 0.25$ as meaningful since the predictor value leads to a great change if it explains over 25% of variance, we set as threshold $R^2 > 0.5$. We then validated the regression by checking the regression quality assumptions such as the normality of residuals, the Homoscedasticity of residuals, the mean of the residuals is zero. The regression quality check was achieved through the *gvlma* (Global Validation of Linear Model Assumptions) package (https://cran.r-project.org/web/packages/gvlma/index.html). Other statistical analyses were performed using additional packages such as *ggplot2*, *deplyr*, *readr, combinat*, etc. from R Foundation 3.2.3 (https://www.r-project.org/foundation/). For forest parameters which can be predicted with R^2 greater than 50%, we generalize the model to the whole forest type and performed the validation with cross-validation (Leave-One-Out Cross-Validation) producing hence the root mean square error (RMSE).
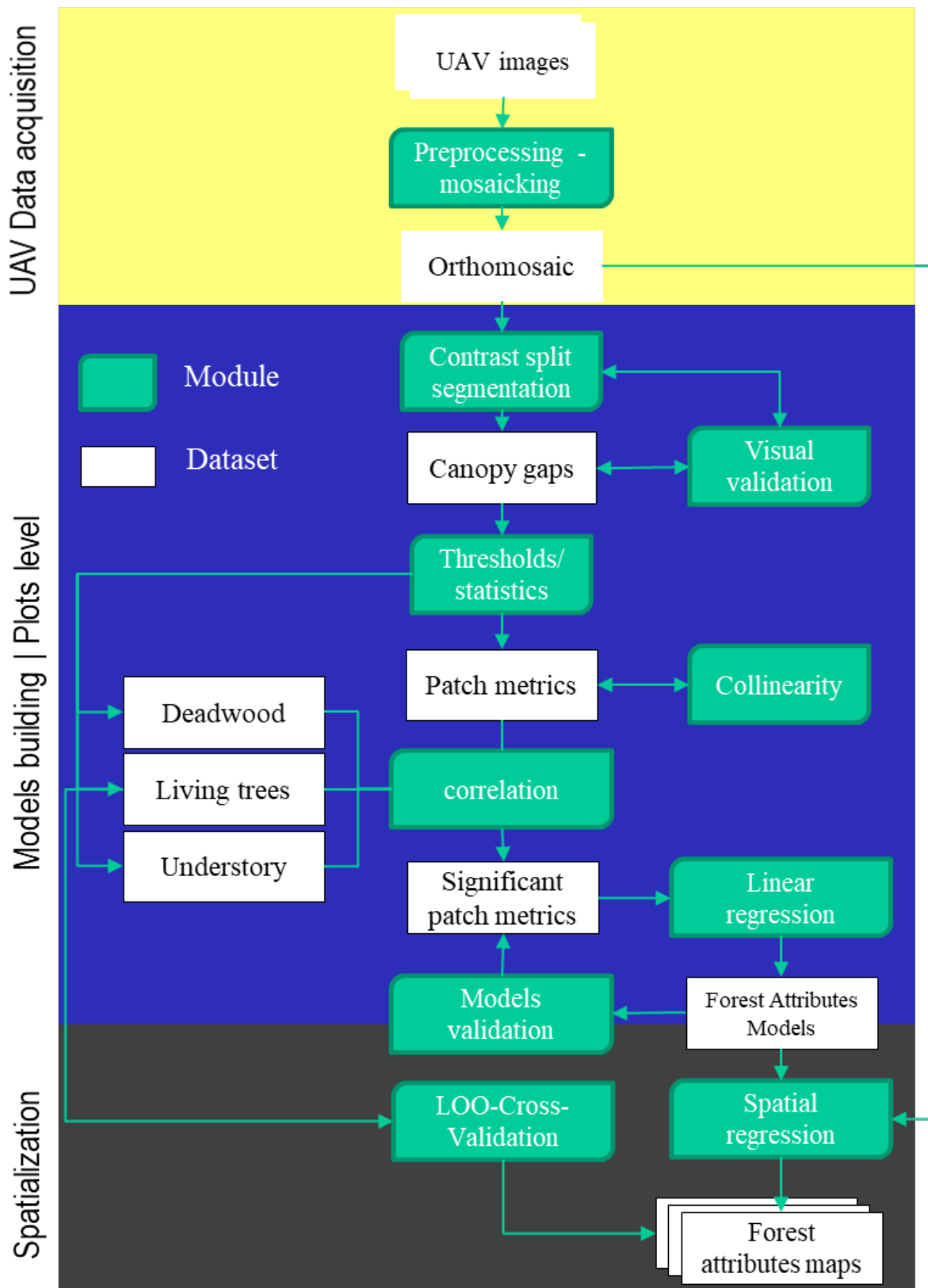
Figure 3-8. Flow chart of the methodology

Chapter 4. RESULTS

4.1. Forest canopy gaps mapping

The contrast split algorithm based on the red band gave the best results. It managed to accurately differentiate dark objects (shaded canopy gaps) to bright ones which, in most cases correspond to the area covered by forest canopy. Gaps detected ranges from 1 pixel (or 100 cm^2) to 122 m^2. Small gaps corresponded indeed to intra-crown gaps while big ones are truly inter-crown gaps. The mapping faithfully delineated shaded canopy gaps but poorly performed in illuminated gaps when the bare soil was apparent (Figure 4-1).
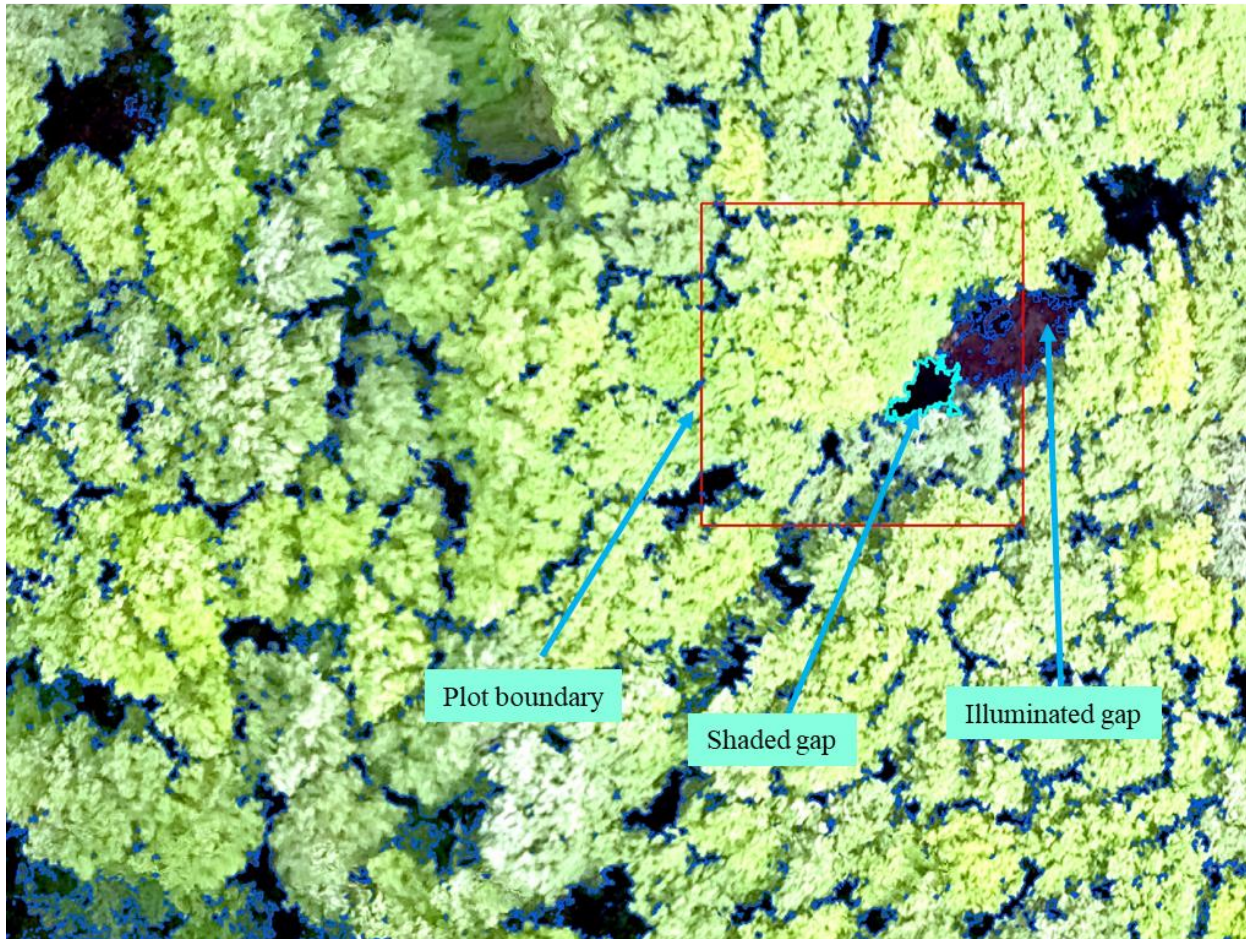
Figure 4-1. Snapshot of gap delineation using the Contrast Split algorithm

The collinearity analysis of gap patch metrics showed that patch metrics are strongly correlated to each other. A sample result of collinearity analysis of the predictor variables is reported in Figure 4-2. There is a high correlation among patch metrics variable. The lowest correlation is obtained with the coefficient of variation, whereas the highest is associated to the sum.
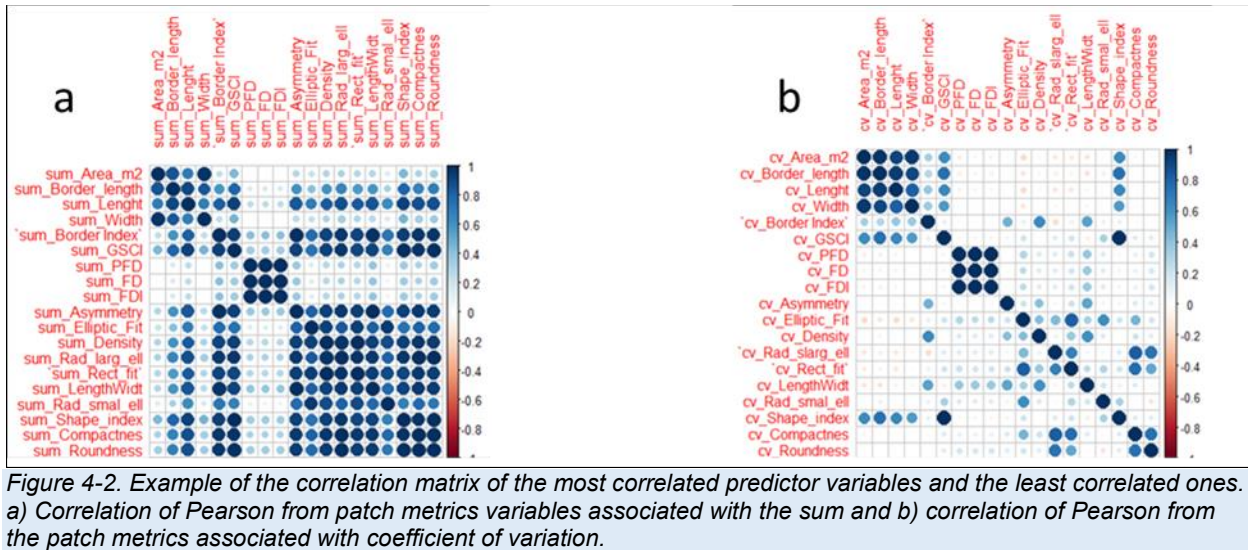
Figure 4-2. Example of the correlation matrix of the most correlated predictor variables and the least correlated ones. a) Correlation of Pearson from patch metrics variables associated with the sum and b) correlation of Pearson from the patch metrics associated with coefficient of variation.

4.2. Understorey analyses

The preliminary analysis reveals that many field parameters related to the understorey data denote a significant difference depending on the forest type. However, Pielou index, MEAN_HTOT and MEAN_DBH do not present any significant difference among the three forest type (Table 4-1 and Figure 4-3). The understorey data is fairly well distributed except in Fagus forest where there are many outliers (Figure 4-3).

Table 4-1. Summary of exploratory statistics on understorey data

Normal distributed variables		
Variables	*ANOVA*	*TUKEY*
I_PIELOU	no significant difference	
MEAN_HTOT	no significant difference	
Variables non normal		
Variables	*KRUSKAL-WALLIS*	*MANN-WHITNEY*
N_PLANTS	***	(1 vs 2)***; (2 vs 3)**
N_SPECIES	***	(1 vs 2)***; (1 vs 3)**
I_SHANNON	***	(1 vs 2)***; (1 vs 3)**
MEAN_DBH	no significant difference	
G_TOT	***	(1 vs 2)***
V_TOT	**	(1 vs 2)**

*p<0,05; ** p<0,01; *** p<0,001; 1 = beech forest; 2 = oak forest; 3 = mixed forest
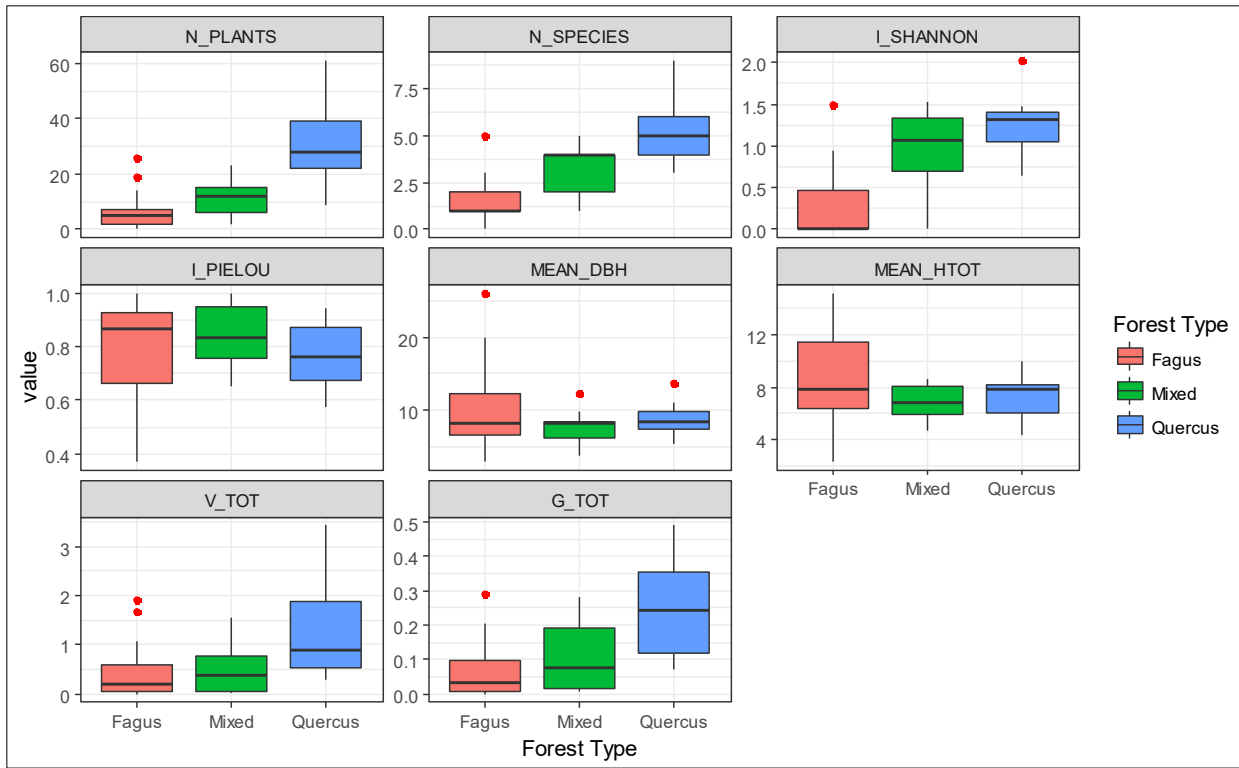
Figure 4-3. Boxplot of the understorey data per forest type

On average Beech forest displays relatively few number of species and number of trees per plots compared to the Oak and the Mixed forests. The oak forest has the highest understorey diversity with around five species per plot. The beech forest has the understorey with the highest basal area and volume per individual plant. This could explain why the number of plant in that forest is relatively lower (Table 4-2).

Table 4-2. Summary of understorey data per forest type

Forest type	Mean number of plants/plot	Mean number of species/plot	Mean basal area (m²)/plant	Mean total volume (m³)/plant
Beech	6,0	1,4	0.011	0.065
Oak	29,9	5,4	0.008	0.042
Mixed	11,7	3,3	0.009	0.046

4.2.1. Correlation analysis of understorey data in Quercus forest

In Quercus forest, there is a significant correlation with both $2m^2$ and $1m^2$ thresholds. Average total height and total basal area were the least correlated with Pearson correlations values of -0.58 and -0.57, respectively. The strongest correlation is between Shannon index and average DBH with values of -0.75 and 0.79, respectively (Table 4-3)

Table 4-3. Coefficient of correlations of Pearson and Spearman for some selected explicative and understorey dependent variables in Quercus forest

	N_PLANTS	N_SPECIES	I_SHANNON	I_PIELOU	MEAN_DBH	MEAN_HTOT	V_TOT	G_TOT
	Mdn_GSCI	Sd_rect.fit	Sd_rect.fit	Sd_Density	Avg_rect fit	Med_B. Index	Med_Asy	Avg_Asy
Threshold	1m^2	2m^2	2m^2	1m^2	1m^2	2m^2	1m^2	1m^2
Pearson	0.73	-0.66	-0.75	-0.64	0.79	-0.58	-0.64	-0.57
Spearman	0.70	-0.73	-0.88	-0.68	0.75	-0.67	-0.57	-0.55

The variability in the number of plants is explained by the median of GSCI with an adjusted R^2 of 0.49, while variabilities in number of species, Shannon index, average DBH are explained by sd_rect.fit (R^2=0.39), sd_rect.fit (R^2=0.52), and sd_rect.fit (R^2=0.60), respectively (Table 4-4 and Table 4-5).

Table 4-4. Results of linear regression of the understorey in Quercus forest

N=13	N_PLANTS B	SE (B)	R^2	p-value		N_SPECIES B	SE (B)	R^2	p-value		I_SHANNON B	SE (B)	R^2	p-value		I_PIELOU B	SE (B)	R^2	p-value
Linear regr.					Linear regr.					Linear regr					Linear regr				
Intercept	-28.85	16.8			Intercept	7.21	0.71		0.000	Intercept	1.70	0.13		0.000	Intercept	1.02	0.10		0.000
Med_GSCI	18.61	5.24	**0.49**	0.005	Sd_rect.fit	-20.66	7.02	**0.39**	0.013	Sd_rect.fit	-4.83	1.28	**0.52**	0.003	Sd_Density	-1.10	0.41	**0.34**	0.021

Table 4-5. Results of linear regression of the understorey in Quercus forest (continuation….)

N=13	MEAN_DBH B	SE (B)	R^2	p-value		MEAN_HTOT B	SE (B)	R^2	p-value		V_TOT B	SE (B)	R^2	p-value		G_TOT B	SE (B)	R^2	p-value
Linear regr.					Linear regr					Linear regr					Linear regr				
Intercept	-23.27	7.38		0.009	Intercept	9.54	1.04			Intercept	5.34	1.48		0.004	Intercept	1.05	0.35		0.012
avg_rect.fit	48.39	11.43	**0.60**	0.001	Mdn_B.Index	-56.61	24.15	**0.27**	0.039	Mdn_Asym.	-6.60	2.36	**0.36**	0.018	Avg_Asym	-1.36	0.59	**0.26**	0.041

4.2.2. Correlation analysis of understorey data in Mixed forest

In Mixed forest, many understorey indicators are strongly correlated with patch metrics. The 2m^2 threshold led to more correlations. The highest positive and negative correlations are obtained with a threshold of 2m^2. The highest positive correlation is between total average height and average Asymmetry with a value of 0.94; whereas the highest negative correlation is between the Number of plants and the average roundness (Table 4-6).

Table 4-6. Coefficient of correlation of Pearson and Spearman for some selected explicative and dependent variables in mixed forest

	N_PLANTS	N_SPECIES	I_SHANNON	I_PIELOU	MEAN_DBH	MEAN_HTOT	G_TOT	V_TOT
	Avg_Round.	Mdn_RSE	Mdn_RSE	avg_RLE	Sum_width	Avg_Asym.	Sd_Asym.	Avg_Comp.
	2m^2	1m^2	1m^2	2 m^2	2m^2	2m^2	2m^2	2m^2
Pearson	-0.81	0.73	0.69	0.71	-0.78	0.94	0.72	-0.67
Spearman	-0.83	0.70	0.70	0.75	-0.70	0.92	0.72	-0.77

RSE= Radius of the Smallest Enclosed Ellipse
RLE=Radius of the Largest Enclosed Ellipse

The goodness of fit of the linear regression to understorey data shows high values. The adjusted-R^2 ranges from 37% to 87% corresponding respectively to total volume (V-TOT) of the understorey and average total height (MEAN_HTOT) (Table 4-7 and Table 4-8).

N=9	B	SE (B)	R²	p-value		B	SE (B)	R²	p-value		B	SE (B)	R²	p-value		B	SE (B)	R²	p-value
		N_PIANTE					N_SPECIES					I_SHANNON					I_PIELOU		
Linear regr.					Linear regr					Linear regr					Linear regr				
Intercept	47.02	9.62		0.002	Intercept	0.86	0.93			Intercept	0.11	0.35			Intercept	0.1	0.3		
avg_Round.	-23.79	6.40	**0.62**	0.007	Med_R.SE	8.29	2.92	**0.47**	0.025	Med_R.SE	2.73	1.08	**0.40**	0.040	avg_R_LE	0.42	0.17	**0.43**	0.045

Table 4-8. Results of Linear regression of the understorey in Mixed forest (continuation….)

N=9	B	SE (B)	R²	p-value		B	SE (B)	R²	p-value		B	SE (B)	R²	p-value		B	SE (B)	R²	p-value
		MEAN_DBH					MEAN_HTOT					G_TOT					V_TOT		
Linear regr.					Linear regr					Linear regr					Linear regr.				
Intercept	9.70	0.82		0.000	Intercept	0.90	0.82			Intercept	-0.02	0.05			Intercept	3.48	1.23		0.026
Sum_width	-0.00	0.00	**0.51**	0.018	Avg_Asym	10.39	1.40	**0.87**	0.000	Sd_Asym.	0.59	0.21	**0.45**	0.027	Avg_Comp	-1.16	0.48	**0.37**	0.048

4.2.3. Correlation analysis of understorey data in Fagus forest

The correlation analysis using an area threshold of $1m^2$ leads to a significance of correlation for the number of species, the Shannon index, the Pielou Index, while the most significant correlation using the $2m^2$ threshold is with the average total height and the coefficient of variation of the Length of the patch metric. The highest correlation is between Pielou index and median of PFD with a correlation of 0.74 and 0.87 for Pearson and Spearman correlations, respectively (Table 4-9).

Table 4-9. Coefficient of correlation of Pearson and Spearman for some selected explicative and dependent variables in Fagus forest

	N_SPECIES	I_SHANNON	I_PIELOU	MEAN_HTOT
	Cv_Round	Sd_Round	Med_PFD	cv_Lenght
Threshold	$1\ m^2$	$1\ m^2$	$1\ m^2$	$2\ m^2$
Pearson	-0.43	0.50	0.74	0.52
Spearman	-0.45	0.56	0.87	0.57

The linear regression fitted to data highlights that up to 48% of variability of the Pielou index can be explained by the median of PFD. Other indicators yielded poor results with only 15% of variability in the number of species explained by the coefficient of variation of the roundness, whereas the Shannon index and the average total height (MEAN_HTOT) variations are accounted from patch metrics by 21% and 23%, respectively (Table 4-10).

Table 4-10. Results of Linear regression of the understorey in Fagus forest

N=28	B	SE (B)	R²	p-value		B	SE (B)	R²	p-value		B	SE (B)	R²	p-value		B	SE (B)	R²	p-value
		N_SPEIES					I_SHANNON					I_PIELOU					MEAN_HTOT		
Linear regr.					Linear regr					Linear regr					Linear regr				
Intercept	3.13	0.77		0.000	Intercept	1.01	0.29		0.002	Intercept	0.26	0.18			Intercept	5.46	1.40		0.000
Cv_Round.	-6.02	2.64	**0.15**	0.033	Sd_Round.	-1.85	0.72	**0.21**	0.018	Med_PFD.	0.06	0.02	**0.48**	0.022	Cv_Length	11.14	4.20	**0.23**	0.016

The spatiatialisation of the understorey models on the extent of the study area underscored some key features. In Quercus forest, Shannon index ranged from just

above 0 to 1.8. These values are in the range of variation of data collected on plots. However, the RMSE of 0.21 seemed a bit too high when reported to values Shannon index can take. The range of variation of MEAN_DBH in Quercus forest is from 2 to 17 cm with an RMSE=1.3 cm. Although the majority of values lies between 2 to 13 cm, the model tends to overestimate the MEAN_DBH since in the plot data we did not have mean BDH exceeding 14 cm.

In Mixed forest, MEAN_HTOT went up to 11 m, with the majority of grids falling between 5 and 9 m. The RMSE was about 0.43 indicating a good prediction with a very low error. The number of plants per grid in the Mixed forest ranged from less than five to 33 with an RMSE of 3.84. this model tended to overestimate the number of plants per grid since the data collected on plots level displayed only a N_PLANTS up to 22. However, in this model, grids exceeding this limit are few (Figure 4-3 and Figure 4-4). We did not perform the spatialization of MEAN_DBH in Mixed forest even though the R2 was greater than 0.5 because the linear model slope was close to zero (Table 4-8). Consequently, there is no big variability in the prediction.
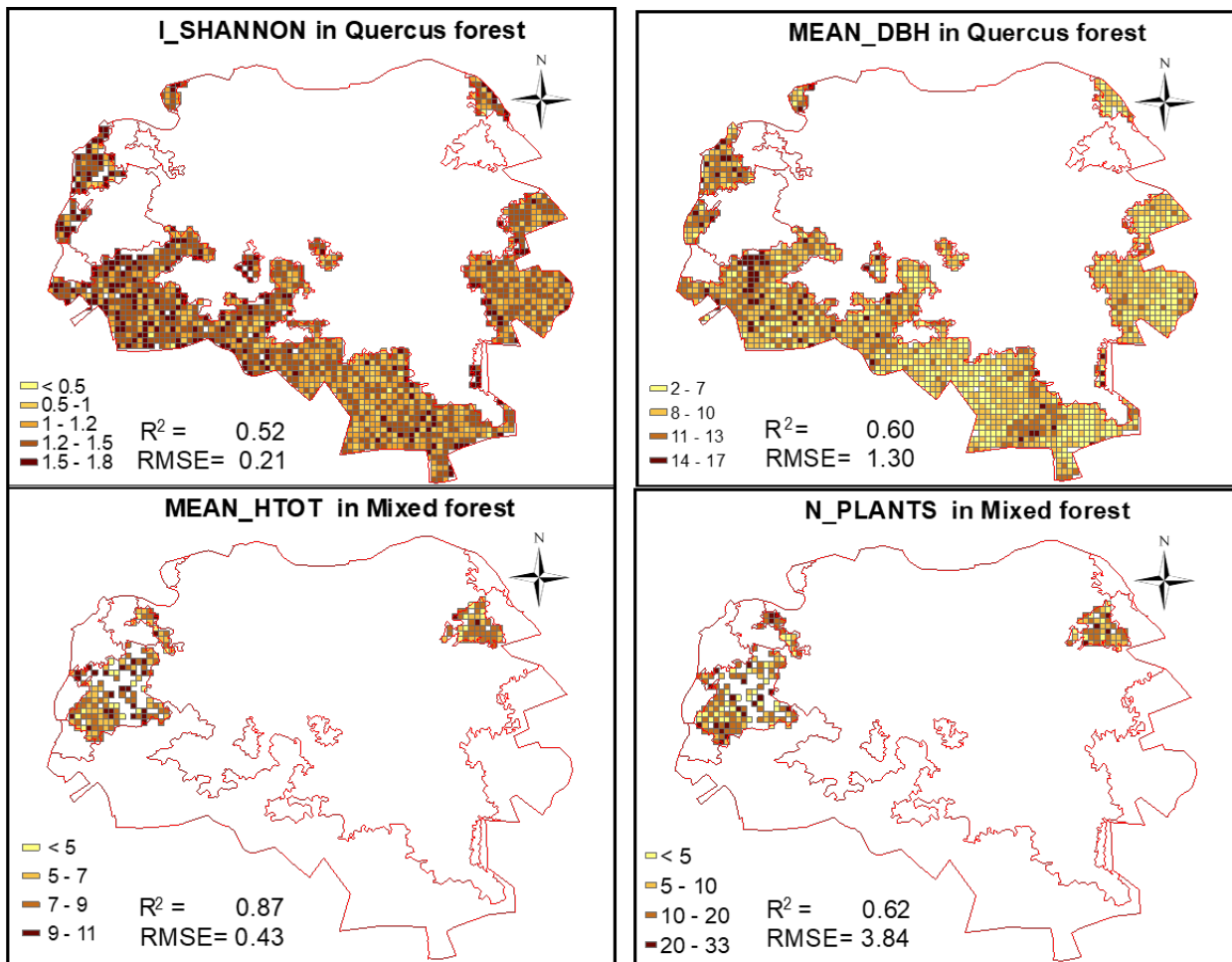
Figure 4-4. Spatialization maps of the understorey data with R^2 greater than 50% in Mixed and Quercus forests

4.3. Living trees

Except for the total basal area (G_TOT) and total volume (V_TOT), all other variables denote significant differences among the three forest types (Table 4-11 and Figure 4-5). The two variables were not further discussed. We focused the analysis on the number of habitats, the percentage of habitat trees and Pretzch index. Living trees data is fairly well distributed in Mixed and Quercus forests. In Fagus forest, the data present some extreme values (Figure 4-5).

Table 4-11. Summary of exploratory statistics on living trees

Variables with normal distribution		
Variables	*ANOVA*	*TUKEY*
N_PLANTS	***	(1 vs 2)***; (2 vs 3)***
I_PRETZSCH	***	(1 vs 2)***; (1 vs 3)***
G_TOT	no significant difference	
V_TOT	no significant difference	
HAB	*	(1 vs 2)**
%_HAB	**	(1 vs 2)*
Non normal distributed variables		
Variables	*KRUSKAL-WALLIS*	*MANN-WHITNEY*
N_SPECIES	***	(1 vs 2)***; (1 vs 3)***
I_MARGALEF	***	(1 vs 2)***; (1 vs 3)***
I_SHANNON	***	(1 vs 2)***; (1 vs 3)***
MEAN_DBH	***	(1 vs 2)***; (2 vs 3)***
MEAN_HTOT	**	(1 vs 2)**

*p<0,05; ** p<0,01; *** p<0,001; 1 = beech forest; 2 = oak forest; 3 = mixed forest
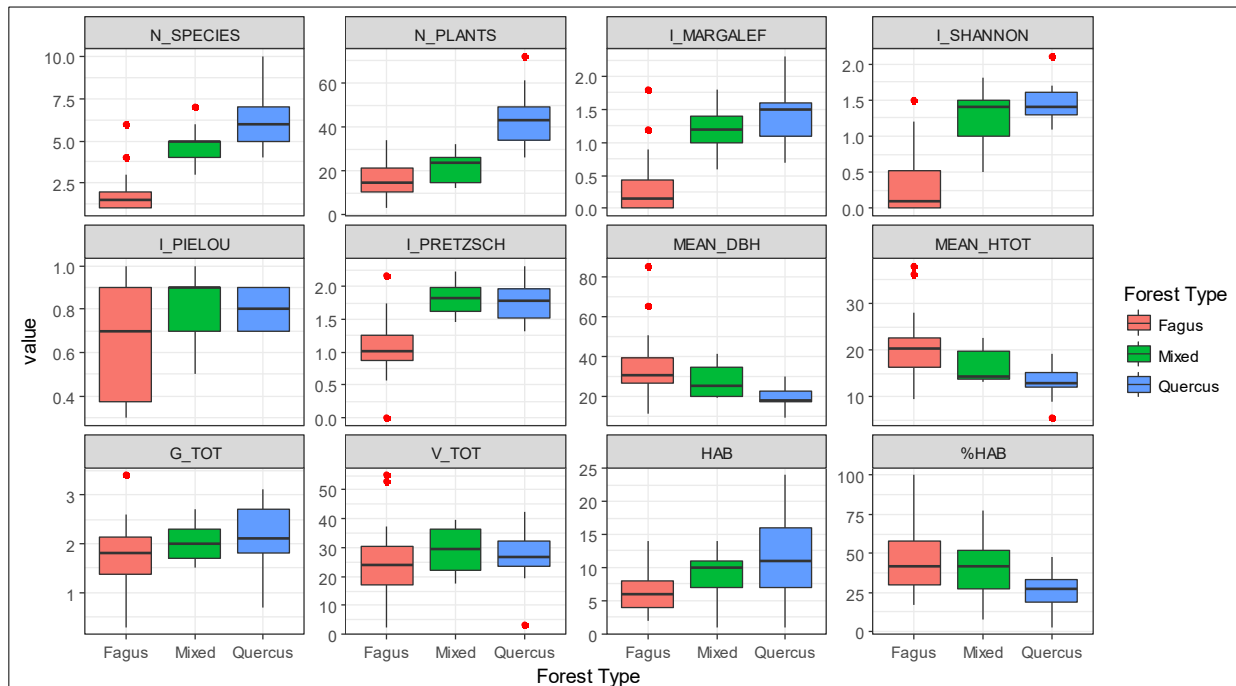
Figure 4-5. Boxplot of the living trees data per forest type

The average number of trees per plot in Fagus forest was only 16 with an average DBH per plot of 35, while Quercus forest depicted an opposite relation; the number of trees was 44 with an average DBH per plot of 19. Mixed forest depicted intermediate results.

Basically, forest stands in Fagus forest although having a larger diameter and height compared to mixed and Quercus forest (Table 4-12) are characterized by a scarcely diversified vertical structure, as reflected by the significantly lower value of the Pretzch index (Figure 4-5).

Table 4-12. Summary of living trees data per plot

Forest type	Mean N_PLANTS	Mean HAB	Mean %_HAB	Mean MEAN_DBH	Mean MEAN_HTOT
Fagus	16	6	47	35	20
Quercus	44	11	25	19	13
Mixed	22	9	42	28	17

4.3.1. Correlation analysis of living trees data in Quercus forest

The use of a $2m^2$ threshold considerably improved correlations. Of the indices on Table 4-13, only MEAN_DBH and MEAN_HTOT produced better results with a $1m^2$ threshold. Pretzsch index yielded the highest correlation with values of -0.87 and -0.90 for Pearson and Spearman correlations, respectively.

Table 4-13. Coefficient of correlations of Pearson and Spearman for some selected explicative and living trees dependent variables in Quercus forest

	N_SPECIES	I_SHANNON	I_MARGALEF	I_PRETZSCH	MEAN_DBH	MEAN_HTOT	HAB	%HAB
	Sd_rect_fit	Cv_Density	Sd_rect_fit	Sd_Density	Sum_rect.fit	Mdn_rect.fit	Sum_rect.fit	Sum_RLE
Threshold	$2m^2$	$2m^2$	$2m^2$	$2m^2$	$1m^2$	$1m^2$	$2m^2$	$2m^2$
Pearson	-0.68	-0.64	-0.71	-0.87	0.61	0.59	-0.79	-0.71
Spearman	-0.72	-0.61	-0.74	-0.90	0.70	0.56	-0.70	-0.64

The goodness of fit in the Quercus forest depicted values ranging from 0.29 to 0.74 corresponding to MEAN_HTOT and I_PRETZSCH, respectively. Up to 59% of variability in the number of habitat trees were explained by sum_Elip.fit, whereas the percentage of habitat trees had a lower adjusted R^2 (R^2 =0.47) (Table 4-14 and Table 4-15).

Table 4-14. Results of linear regression of living trees data in Quercus forest

N_SPECIES	B	SE (B)	R^2	p-value	I_SHANNON	B	SE (B)	R^2	p-value	I_MARGLEF	B	SE (B)	R^2	p-value	I_PRETZSCH	B	SE (B)	R^2	p-value
N=13																			
Linear regr.					Linear regr					Linear regr					Linear regr				
Intercept	8.13	0.71		0.000	Intercept	1.81	0.14		0.000	Intercept	1.94	0.18		0.000	Intercept	2.32	0.1		0.000
Sd_rect_fit	-21.46	7.04	**0.41**	0.011	Cv_Density	-2.61	0.95	**0.35**	0.019	Sd_rect_fit	-6..02	1.80	**0.46**	0.006	Sd_Density	-2.68	0.45	**0.74**	0.000

Table 4-15. Results of linear regression of living trees data in Quercus forest (continuation….)

MEAN_DBH	B	SE (B)	R^2	p-value	MEAN_HTOT	B	SE (B)	R^2	p-value	HAB	B	SE (B)	R^2	p-value	%HAB	B	SE (B)	R^2	p-value
N=13																			
Linear regr.					Linear regr					Linear regr					Linear regr				
Intercept	11.30	3.42		0.007	Intercept	-15.73	11.99			Intercept	20.54	2.44		0.000	Intercept	41.87	5.45		0.000
Sum_rect.fit	1.29	0.50	**0.32**	0.02	Mdn_rect.fit	45.41	18.68	**0.29**	0.033	Sum_rect.fit	-3.10	0.73	**0.59**	0.001	Sum_RLE	-1.86	0.54	**0.47**	0.006

4.3.2. Correlation analysis of living trees data in Mixed forest

In mixed forest, only four indices showed a strong correlation with patch metrics. Apart MEAN_DBH, which depicted a positive correlation, the three other indices were

negatively correlated with a select patch metrics. The number of habitat trees (HAB) produced the highest correlation with a value of 0.90 for Pearson correlation and 0.92 for Spearman correlation (Table 4-16).

Table 4-16. Coefficient of correlations of Pearson and Spearman for some selected explicative and living trees dependent variables in Mixed forest

	MEAN_DBH	MEAN_HTOT	HAB	%HAB
	Avg_Round.	Sd_Asym.	Cv_Length	Avg_RSE
Threshold	$2m^2$	$1m^2$	$2m^2$	$1m^2$
Pearson	0.74	-0.84	-0.90	-0.83
Spearman	0.82	-0.95	-0.92	-0.92

Variabilities in HAB, %HAB, MEAN_HTOT, and MEAN_DBH are explained at 79%, 64%, 67% and 49% by cv_length, avg_RSE, sd_Asym and avg_Round, respectively (Table 4-17).

Table 4-17. Results of linear regression of living trees data in Mixed forest

MEAN_DBH					MEAN_HTOT					HAB					%HAB				
N=9	B	SE (B)	R^2	p-value		B	SE (B)	R^2	p-value		B	SE (B)	R^2	p-value		B	SE (B)	R^2	p-value
Linear regr.					Linear regr					Linear regr					Linear regr				
Intercept	-10.86	13.32			Intercept	27.74	2.70		0.000	Intercept	14.34	1.20		0.000	Intercept	108.24	17.54		0.000
Avg_Round	25.92	8.86	**0.49**	0.022	Sd_Asym.	-49.06	11.72	**0.67**	0.004	Cv_Length	-14.01	2.51	**0.79**	0.000	Avg_RSE	-208.99	53.19	**0.64**	0.005

4.3.3. Correlation analysis of living trees data in the Fagus forest

The correlation is only obtained with the threshold of $2m^2$. HAB and %HAB were the only indices that depicted a correlation although weak with values not exceeding 0.50 (Table 4-18).

Table 4-18. Coefficient of correlations of Pearson and Spearman for some selected explicative and living trees dependent variables in Fagus forest

2m	HAB	%HAB
	cv_PFD	Avg_RSE
Pearson	0.43	-0.38
Spearman	0.50	-0.39

Variabilities in HAB and %HAB explained by the linear regression models presented in Table 4-19 are low. The percentage explained remains 15% for HAB and 11% for %HAB.

Table 4-19. Results of linear regression of living trees data in Fagus forest

HAB					%HAB				
N=28	B	SE (B)	R^2	p-value		B	SE (B)	R^2	p-value
Linear regr.					Linear regr				
Intercept	4.00	1.21		0.003	Intercept	61.35	7.88		0.000
cv_PFD	11.82	5.23	**0.15**	0.034	Avg_RSE	-58.21	27.71	**0.11**	0.045

The generalization of regression models obtained is presented in Figure 3-1. In Quercus forest, I_PRETZSCH varied from 1 to 2.4 with RMSE of 0.40. The majority of grids had the index higher than 1.7 indicating a complex vertical structure. The range of variation of the index is in accordance with the field data collected on plots. In the same forest type,

the number of habitat trees reached 20 with RMSE of 3.89. The western side of the forest has more forest habitat trees than the eastern side.
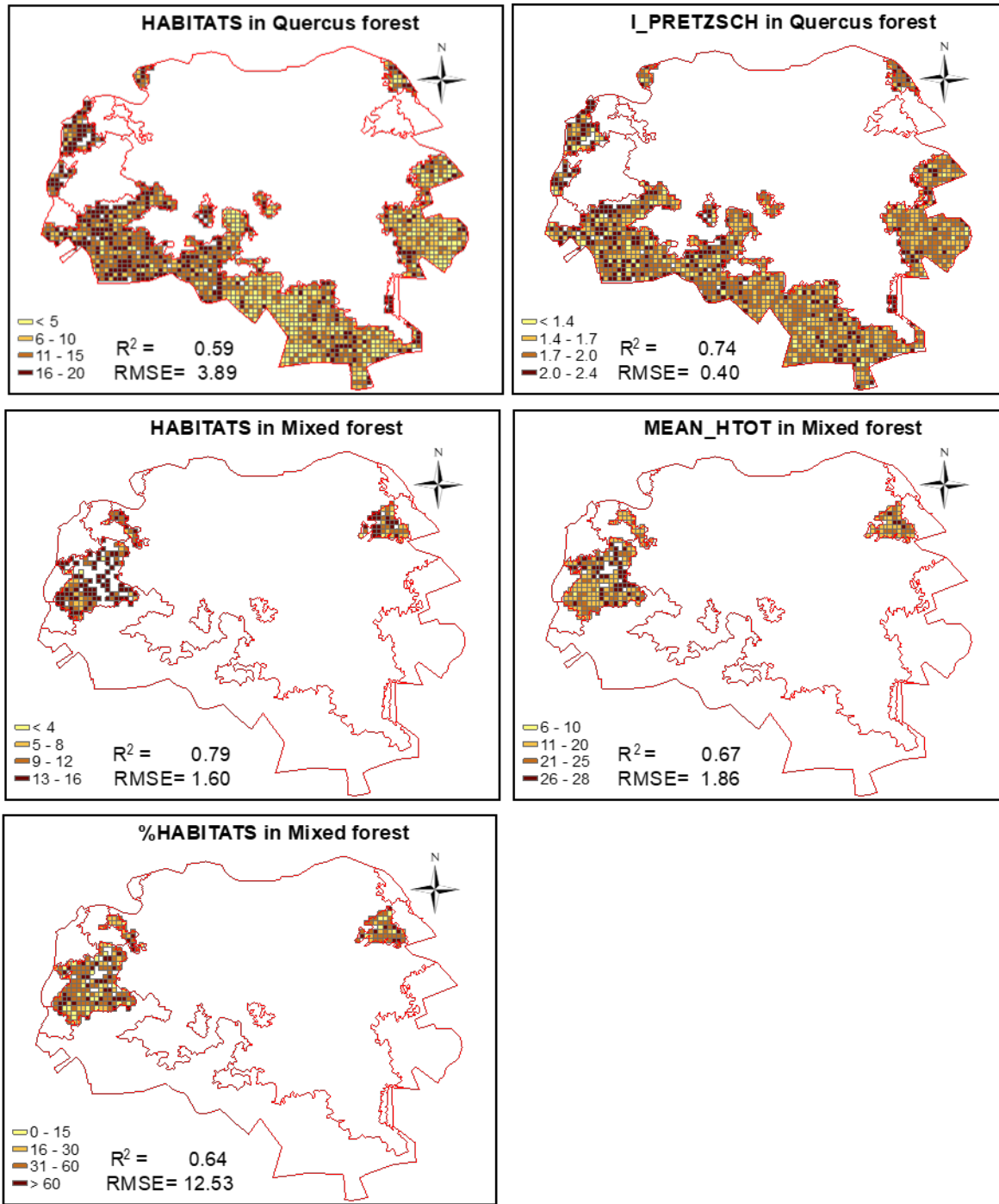
Figure 4-6. Spatialization of living trees parameters with R^2 greater than 50% in Mixed and Quercus forests

In Mixed forest, the majority of grids had a number of habitat trees higher than 9. In this forest, the prediction error is relatively smaller with an RMSE of 1.6. the percentage of habitat trees per grid is more variable with values ranging from 0 to 100%. The model added more variability than the one observed on plots level. The MEAN_HTOT varied

from 6 to 28 m with an RMSE of 1.86. An error that can be considered as low. However, the range of values of the MEAN_HTOT in the whole forest is larger than the one observed on plots level where the range was 12 to 23 m.

4.4. Deadwood

4.4.1. Exploratory analysis

There is no difference among lying deadwood, standing deadwood and stumps in different forest types. Similarly, the volume of deadwood by decay class is not significantly different in different forest types. The deadwood volume is highly skewed with many nil values. Although the Figure 4-7 shows that there are many outliers, the field survey proved that there are actual plots with high deadwood while there are some plots with no deadwood at all. Therefore, it is misleading to consider these plots as outliers. A square root transformation improved the data distribution by reducing the skewness particularly with the total lying deadwood, the total standing deadwood, total deadwood, VOL1, VOL3 and VOL4 (Figure 4-7).
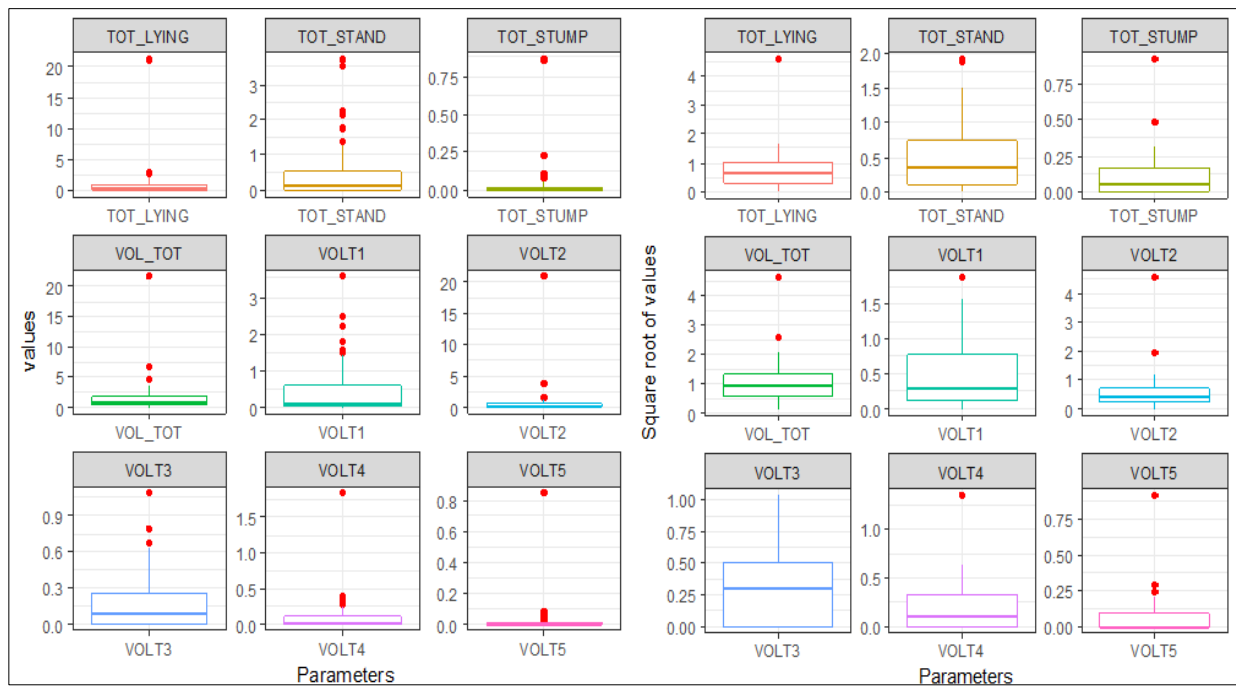
Figure 4-7. Boxplot chart of the deadwood data. On the left, the natural values and on the right the square root transformation

4.4.2. Correlation analysis

Total lying deadwood, total stumps, total standing deadwood, and VOL1, VOL2, and the total volume of deadwood in the plot are significantly correlated with gap patch metrics (Table 4-20). The strongest correlation is in total lying deadwood and the weakest one is found in VOL1.

33

Table 4-20. Coefficient of correlation of Pearson and Spearman associated to the deadwood

	TOT_LYING	TOT_STUMP	TOT_STAND	VOL1	VOL2	VOL_TOT
	Sd_GSCI	Cv_Density	Sd_FD	Sd_FD	Cv_GSCI	Cv_GSCI
Threshold	$1m^2$	$1m^2$	$2m^2$	$2m^2$	$1m^2$	$1m^2$
Pearson	-0.53	-0.30	-0.41	-0.33	-0.42	-0.39
Spearman	-0.46	-0.34	-39	-0.30	-0.37	-0.34

The regression analysis and its assumptions verification showed that none of the deadwood parameters fully satisfies the linear regression assumptions. For instance, TOT_STAND violates the skewness assumption and VOL_TOT violates all the assumptions, namely independence of residuals, homoscedasticity and residuals normally distributed (skewness and Kurtosis).

Chapter 5. DISCUSSIONS

5.1. Mapping forest canopy gaps

Gap mapping from UAV RGB 10 cm resolution images seems to produce very promising results. In this study, we accomplished mapping gaps as small as one pixel corresponding in fact to intra-canopy openings. This very high spatial resolution mapping of gaps is important because some ecological phenomena, such as understorey structure dependencies, are only quantifiable if small gaps are taken into account. Since there is not yet a rule for minimum gap size, different authors set, arbitrarily a minimum gap size of 1m^2 (Getzin, Wiegand, and Schöning 2012; Getzin, Nuske, and Wiegand 2014; Boyd et al. 2013; Busing 1994), 5 m^2 (Vepakomma, St-Onge, and Kneeshaw 2008), 10 m^2 (Schliemann and Bockheim 2011; Zielewska-Büttner, Adler, Ehmann, et al. 2016a) and 50 m^2 (Bonnet et al. 2015). To circumvent this lack in the literature, we did not set any gap size limit but let the ecological phenomenon under investigation dictates the gap size limit relevant. Hobi et al. (2015) used the same approach by not setting any gap size limit. The gap mapping used in this paper does not take into account the vegetation height. Therefore, our mapping, although consistent with the definition given by Brokaw (1982), focusses only on shaded gaps or dark objects. Zielewska-Büttner, Adler, Ehmann, et al. (2016) reported as well that in their attempt to map forest canopy gaps, the shadow occurrence and forest height affected the mapping accuracy.

Many other authors who mapped forest gaps from remote sensing point of view used either the LiDAR-derived forest canopy model (Boyd et al. 2013), or RGB imagery photogrammetric derived CHM (Zielewska-Büttner, Adler, Ehmann, et al. 2016b; Zielewska-Büttner, Adler, Petersen, et al. 2016; Betts, Brown, and Stewart 2005). Alternatively, fish eye (Perroy, Sullivan, and Stephenson 2017), or terrestrial laser can be used. All those techniques, although effective, are not affordable for small forest land owners.

Furthermore, the forest canopy mapping was highly affected by the quality of the orthomosaic and images acquisition conditions. In this study, the orthomosaic coregistration presented some flaws in certain areas. Those areas denoted a low quality in gaps delineation and even in the visual interpretation of what constitutes a gap. The second limitation came from the difference in reflectance between the dataset acquired in the two consecutive days. Although the images were acquired at noon to reduce the bidirectional reflectance effect (Lehmann et al. 2015), the sun illumination between the two days was not the same; leading thus to two set of images with slightly different brightness.

In addition, the eBee NIR image presented a serious limitation in its use for mapping forest canopy gaps. As shown in Figure 3-5, the camera is less sensible in near infrared channel compared to the red and the green channels. In fact, the near infrared sensibility of the camera covers as well the whole visible range. Consequently, the near infrared channel constitutes one kind of panchromatic extending to near infrared region. Besides this spectral resolution deficiency, the NIR camera data has a spatial resolution of 20 cm compared to 10 cm for the RGB. As result, the NIR camera data was not of great utility we hypothesized beforehand.

Finally, the contrast split algorithm utilized here with the reference layer being the red band separated dark objects from bright ones based on the reflectance of image objects. However, the algorithm failed to detect illuminated canopy gaps where the bare soil is visible because the bare soil reflectance is as high as the one of the vegetation. Therefore, the algorithm missed big gaps with no vegetation but with apparent bare soil.

5.2. Assessing understorey through forest canopy gaps

Overall, mixed forest yielded the best results (Figure 5-1). It showed a significant correlation with almost all indices. The highest adjusted R^2 was as well obtained in Mixed forest with a value of 0.87. Fagus forest underperformed the two other forest types. In mixed forest, only three indices had shown a significant correlation, namely MEAN_HTOT, MEAN_DBH, , and N_PLANTS. Intermediate results were obtained in Quercus forest in which the adjusted R^2 obtained were relatively lower compared to results in mixed forest except for MEAN_DBH and I_SHANNON. The regression with five field parameters (MEAN_HTOT, MEAN_DBH, , and N_PLANTS in Mixed forest, and MEAN_DBH and I_SHANNON in Quercus forest) exceeded the threshold of adjusted R^2 of 0.5 (Figure 5-1).
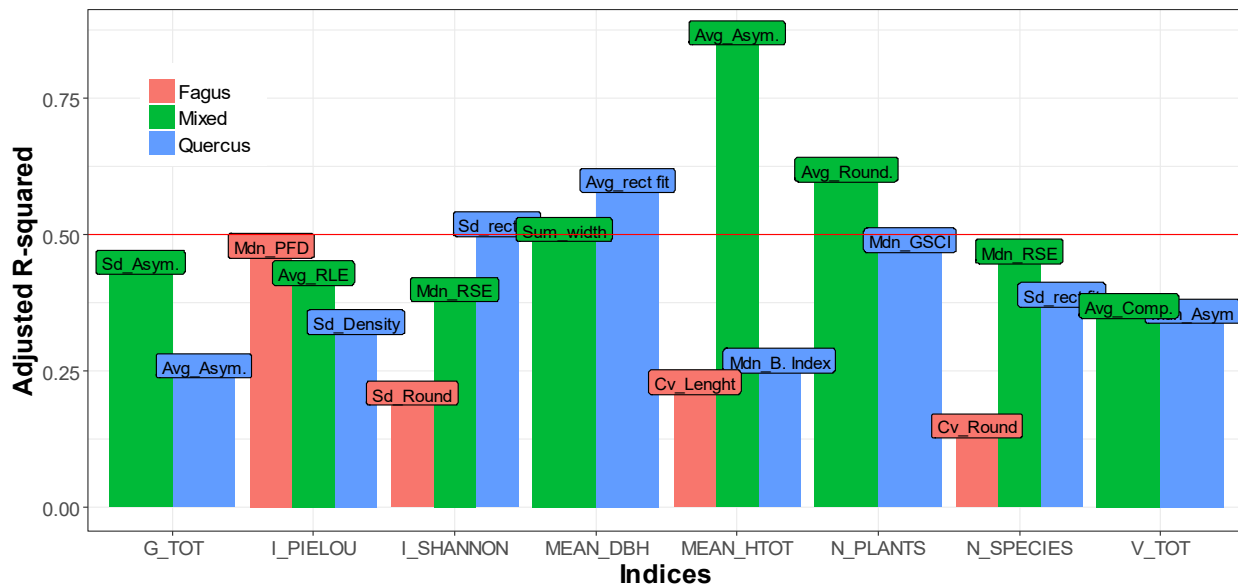

Figure 5-1. Summary bar chart of adjusted R^2 from linear regression with understorey data in all the three forest types

Forest canopy gaps is a good proxy for assessing forest horizontal structure such as N_PLANTS, N_SPECIES, I_SHANNON, I_PIELOU, MEAN_DBH, and G_TOT of forest understorey. The number of species was negatively correlated with patch metrics in both Fagus and Quercus forests but was positively correlated in mixed forest. And finally, an increase in RSE means a proportional increase in the number of species in mixed forest. In fact, the big radius of smallest enclosed ellipse indicates that the gap patch itself is big and therefore open to light to allow development of understorey species.

The number of plants in both Quercus and Mixed forests can be assessed respectively by the mdn_GSCI and avg_Round. The correlation between gap metrics and understory in Fagus forest might not have been significant because of the lower vertical structural diversification of this forest type in the examined conditions. In mixed forest, the number

of plants decreased when gaps have shapes differing from an ellipse, whereas in Quercus forest, more complex shapes of gaps led to more number of species. The result in mixed forest is quite unexpected since more complex shapes (an ellipse is a regular shape) should be associated with more horizontal structure richness. The understorey diversity indicators (I_PIELOU and I_SHANNON) were strongly correlated with patch metrics in the three types of forest.

The canopy gaps patch metrics can be distinguished into two groups; the ones informing on the shape of the gap and the ones referring to the extent. Of the patch metrics correlated to the understorey parameters, only Cv_Length is extent related patch metric. This suggests that the shape of the gap has more effect on the understory than its extent solely. This finding must be taken into account when silviculture activities aim to mimic natural gap creation so to trigger forest dynamics in managed forests. Despite this findings, many authors have only focused on mapping forest canopy gaps' size and their spatial distribution. For instance, Garbarino et al. (2012) and Hobi et al. (2015) mapped gaps' size and their distribution from satellite imagery, whereas Zielewska-Büttner, Adler, Ehmann, et al. (2016b) did the same study using CHM.

5.3. Assessing living trees through forest canopy gaps

In mixed forest, only four indices were correlated with patch metrics compared to Quercus forest where all indices are correlated. However, adjusted R^2 values outperformed in mixed forest with values ranging from 0.49 to 0.79. The performance of linear regression is the lowest in Fagus forest. In Mixed forest, three of the correlated parameters namely, %HAB, HAB, and MEAN_HTOT exceeded the threshold of $R^2 > 0.5$. The two field parameters in Quercus forest that were best correlated to gap metrics were the number of habitat (HAB) and total mean height (MEAN_HTOT) (Figure 5-2).
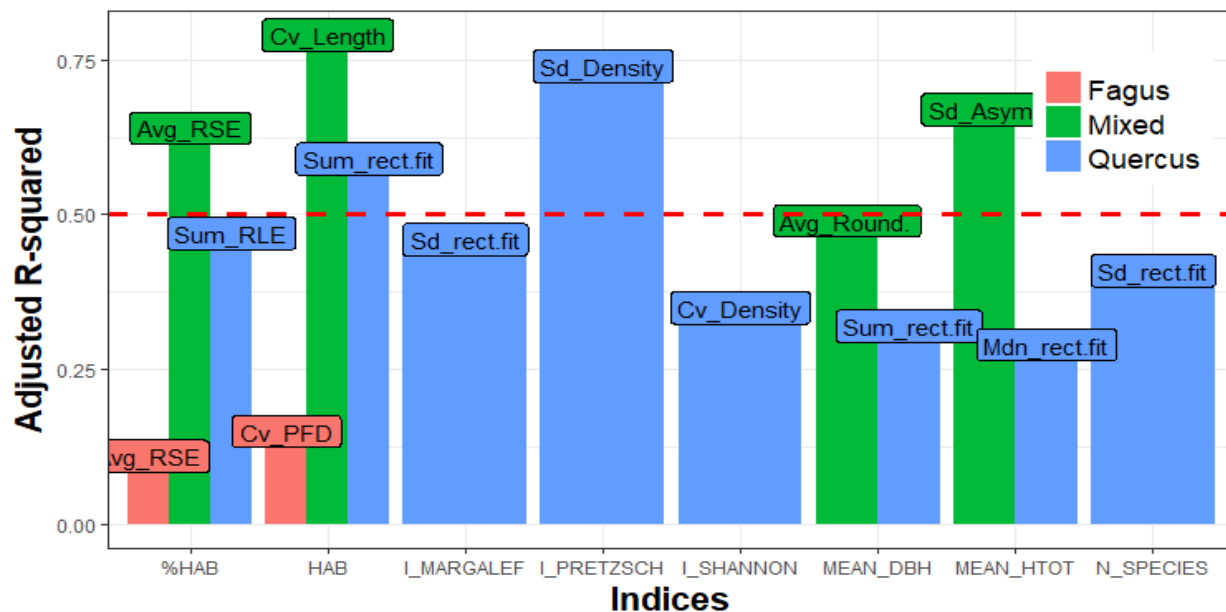

Figure 5-2. Summary bar chart of adjusted R^2 from linear regression with living trees data in all the three forest types

The number of habitat trees and their percentage are functional forest ecosystems attributes and are considered difficult to measure directly (Franklin et al. 2002) particularly

using remote sensing. These two attributes proved they could be assessed using the forest canopy gaps as a surrogate variable. In fact, habitat trees, which are old large trees, create a structural diversity because of their multiple and dead tops, bole and top decays. This specific structure influences the canopy arrangement and creates, therefore, small canopy gaps with specific patch metrics that can be used as a footprint of habitat trees. The only field parameters in Fagus forest correlated with gap patch metrics were the number of habitat trees and their percentage because it is only habitat trees (e.g. sanags, broken or partially dead crown) that cause perforation in the canopy layer of that forest type at this early development stage.

In addition, in general, results were poor in Fagus forest because of the plot size. Fagus forest was constituted with few and big trees per plot. These horizontal and vertical structures make it impossible to observe a great variety of canopy gaps, where present, in a plot of only 529 m^2. In their study, Getzin, Wiegand, and Schöning (2012) used plots of one (1) hectare which is much larger (almost twenty times bigger) than the plot size in this study.

Similarly, poor results obtained for the deadwood could be explained by the fact that on one hand, forest canopy gaps explored in this study are not necessary gaps due to the death of trees but can just be gaps created by the spatial arrangement of the canopy layer due to trees shape. On the other hand, the quantity of deadwood found in plots itself is low with some plots missing some categories of deadwood. This low variability in the collected deadwood makes correlation analysis less feasible.

Chapter 6. CONCLUSIONS AND RECOMMENDATIONS

The main aim of this study was to map forest canopy gaps on small scale level and assess how some forest parameters could be assessed using solely forest canopy gaps shape and extent metrics extracted from UAV RGB imagery. Forest canopy openings were faithfully extracted from the 10cm spatial resolution UAV RGB orthomosaic. The mapping performed relatively poorly when the gap was illuminated with the bare soil being apparent.

The forest canopy gap patch metrics (which inform on the size and the shape of canopy gaps within a square grid of 23 m of side) were strongly collinear. They showed a strong correlation with the field data especially in the understory and the living trees. For understory data, five field parameters depicted an R^2 greater than 0.5 with the highest being equal to 0.87. Results were better in mixed forest followed by Quercus forest while poor results were obtained in Fagus forest.

Similarly, the living tree data yielded results comparable to the understorey data. Many correlations were observed between the field parameters and the gap patch metrics. About five field parameter led to an R^2 greater than 0.5. Of the living data parameters, the number of habitat trees in mixed forest had the highest R^2 with a value of 0.79. In Fagus forest, only the number of habitat trees and the percentage of habitat trees showed a correlation. The number of field parameters with high correlations in Quercus forest is higher than the one in mixed forest.

The model failed to predict the deadwood as a whole, by deadwood components or separated into decay classes. As a general remark, most patch metrics that depicted considerable correlation with field parameter in both living trees and understorey data, were shape related patch metrics.

The spatialization of the forest field parameters models in both Quercus and Mixed forests for the understorey and living trees data underscored the models validity with low RMSEs although in some cases the model tended to introduce more variability in data than the one observed on plots.

Final recommendations for replicating and improving the methodological approach in other test sites are:

[1] In general, the forest canopy mapping could be improved by integrating the NIR band; thus the panchromatic layer should be narrowed.
[2] The collection of the RBG data should be done within the same day with a short duration.
[3] The field data should be collected on plots bigger than 529 m^2 in order to include more variability and integrate big gaps which may give better insight for forest types such as Fagus forest, especially when entering older development stages typically characterized by gap formation, and significant development of new vegetation in the understory.

REFERENCES

Anderson, Karen, and Kevin J. Gaston. 2013. "Lightweight Unmanned Aerial Vehicles Will Revolutionize Spatial Ecology." *Frontiers in Ecology and the Environment* 11 (3): 138–46. doi:10.1890/120150.

Anonymous. 2017. "E-Bee." https://www.sensefly.com/.

Assmann, Ernst. 1970. *The Principles of Forest Yield Study*. Pergamon Press. Oxford.

Barden, Lawrence S. 1981. "Forest Development in Canopy Gaps of a Diverse Hardwood Forest of the Southern Appalachian Mountains." *Oikos* 37 (2): 205. doi:10.2307/3544466.

Belgiu, Mariana, and Lucian Drăgu. 2016. "Random Forest in Remote Sensing: A Review of Applications and Future Directions." *ISPRS Journal of Photogrammetry and Remote Sensing* 114: 24–31. doi:10.1016/j.isprsjprs.2016.01.011.

Betts, Harley D, Len J Brown, and Glenn H Stewart. 2005. "Forest Canopy Gap Detection and Characterisation by the Use of High- Resolution Digital Elevation Models." *New Zealand Journal of Ecology* 29 (1). Zealand Ecological Society: 95–103. http://www.nzes.org.nz/nzje.

Bonnet, Stéphanie, Rachel Gaulton, François Lehaire, and Philippe Lejeune. 2015. "Canopy Gap Mapping from Airborne Laser Scanning: An Assessment of the Positional and Geometrical Accuracy." *Remote Sensing* 7 (9): 11267–94. doi:10.3390/rs70911267.

Boyd, Doreen S, Ross A Hill, Chris Hopkinson, and Timothy R Baker. 2013. "Landscape-Scale Forest Disturbance Regimes in Southern Peruvian." *Ecological Applications* 23 (7): 1588–1602. http://www.jstor.org/stable/23596784 Accessed:

Brokaw, Nicholas V. L. 1982. "The Definition of Treefall Gap and Its Effect on Measures of Forest Dynamics." *Biotropica* 14 (2): 158. doi:10.2307/2387750.

Bunting, Peter, and Richard Lucas. 2006. "The Delineation of Tree Crowns in Australian Mixed Species Forests Using Hyperspectral Compact Airborne Spectrographic Imager (CASI) Data." *Remote Sensing of Environment* 101 (2): 230–48. doi:10.1016/j.rse.2005.12.015.

Bunting, Peter, Richard M. Lucas, Kerstin Jones, and Anthony R. Bean. 2010. "Characterisation and Mapping of Forest Communities by Clustering Individual Tree Crowns." *Remote Sensing of Environment* 114 (11). Elsevier Inc.: 2536–47. doi:10.1016/j.rse.2010.05.030.

Busing, R T. 1994. "Canopy Cover and Tree Regeneration in Old-Growth Cove Forests of the Appalachian Mountains." *Vegetatio* 115: 19–27. https://andrewsforest.oregonstate.edu/sites/default/files/lter/pubs/pdf/pub1808.pdf.

Bustamante, Luis Antonio Esquivel. 2015. *Forest Monitoring with Drones : Application Strategies for Protected Riverine Forest Ecosystems in the Atlantic Forest of Rio de*. TH KÖLN (UNIVERSITY OF APPLIED SCIENCES) MASTER THESIS.

Bütler, Rita, Thibault Lachat, Laurent Larrieu, and Yoan Paillet. 2013. "Habitat Trees : Key Elements for Forest Biodiversity." In *Integrative Approaches as an Opportunity for the Conservation of Forest Biodiversity*, edited by D. Kraus and F. Krumm, European F, 84–91. http://www.efi.int/files/attachments/publications/integrate_2013.pdf.

Candiago, Sebastian, Fabio Remondino, Michaela De Giglio, Marco Dubbini, and Mario Gattelli. 2015. "Evaluating Multispectral Images and Vegetation Indices for Precision Farming Applications from UAV Images." *Remote Sensing* 7 (Vi): 4026–47. doi:10.3390/rs70404026.

Castedo-Dorado, Fernando, Gorka Lago-Parra, Maria J. Lombardero, Andrew M. Liebhold, and Maria F. Alvarez-Taboada. 2016. "European Gypsy Moth (Lymantria Dispar Dispar L.) Completes Development and Defoliates Exotic Radiata Pine Plantations in Spain." *New Zealand Journal of Forestry Science* 46 (1). New Zealand Journal of Forestry Science. doi:10.1186/s40490-016-0074-y.

Chianucci, Francesco, Leonardo Disperati, Donatella Guzzi, Daniele Bianchini, Vanni Nardino, Cinzia Lastri, Andrea Rindinella, and Piermaria Corona. 2016. "Estimation of Canopy Attributes in Beech Forests Using True Colour Digital Images from a Small Fixed-Wing UAV." *International Journal of Applied Earth Observation and Geoinformation* 47. Elsevier B.V.: 60–68. doi:10.1016/j.jag.2015.12.005.

Clifford, H. T. (Harold Trevor), and William Stephenson. 1975. *An Introduction to Numerical Classification*. Academic Press. http://www.sciencedirect.com/science/book/9780121767501.

Colomina, I., and P. Molina. 2014. "Unmanned Aerial Systems for Photogrammetry and Remote Sensing: A Review." *Journal of Photogrammetry and Remote Sensing* 7 (8). Springer Netherlands: 9632–54. doi:10.1016/j.isprsjprs.2014.02.013.

Corona, Piermaria. 2010. "Integration of Forest Mapping and Inventory to Support Forest Management." *IForest* 3 (MAY): 59–64. doi:10.3832/ifor0531-003.

Corona, Piermaria, Gherardo Chirici, Ronald E. McRoberts, Susanne Winter, and Anna Barbati. 2011. "Contribution of Large-Scale Forest Inventories to Biodiversity Assessment and Monitoring." *Forest Ecology and Management* 262 (11). Elsevier B.V.: 2061–69. doi:10.1016/j.foreco.2011.08.044.

Crowther, T W, H B Glick, K R Covey, C Bettigole, D S Maynard, S M Thomas, J R Smith, et al. 2015. "Mapping Tree Density at a Global Scale." *Nature* 525 (7568): 201–5. doi:10.1038/nature14967.

Czapski, Paweł, Mariusz Kacprzak, Jan Kotlarz, Karol Mrowiec, Katarzyna Kubiak, and Miłosz Tkaczyk. 2015. "Preliminary Analysis of the Forest Health State Based on Multispectral Images Acquired by Unmanned Aerial Vehicle." *Folia Forestalia Polonica* 57 (3): 138–44. doi:10.1515/ffp-2015-0014.

Dandois, Jonathan P., and Erle C. Ellis. 2013. "High Spatial Resolution Three-Dimensional Mapping of Vegetation Spectral Dynamics Using Computer Vision." *Remote Sensing of Environment* 136. The Authors: 259–76. doi:10.1016/j.rse.2013.04.005.

Del Pozo, Susana, Pablo Rodriguez-Gonzalvez, David Hernandez-Lopez, and Beatriz Felipe-Garcia. 2014. "Vicarious Radiometric Calibration of a Multispectral Camera on Board an Unmanned Aerial System." *Remote Sensing* 6 (3): 1918–37. doi:10.3390/rs6031918.

Dezso, Balázs, István Fekete, Dávid Gera, Roberto Giachetta, István László, András Benczúr, B Dezs″, et al. 2012. "OBJECT-BASED IMAGE ANALYSIS IN REMOTE SENSING APPLICATIONS USING VARIOUS SEGMENTATION TECHNIQUES." *Annales Univ. Sci. Budapest., Sect. Comp* 37: 103–20. http://ac.inf.elte.hu/Vol_037_2012/103_37.pdf.

Díaz-Varela, Ramón, Raúl de la Rosa, Lorenzo León, and Pablo Zarco-Tejada. 2015. "High-Resolution Airborne UAV Imagery to Assess Olive Tree Crown Parameters Using 3D Photo Reconstruction: Application in Breeding Trials." *Remote Sensing* 7: 4213–32. doi:10.3390/rs70404213.

Drauschke, M, J Bartelsen, and P Reidelstürz. 2014. "Towards Uav-Based Forest Monitoring." *Proceedings of the Workshop on UAV-Basaed Remote Sensing Methods for Monitoring Vegetation* 94: 21–32. doi:10.5880/TR32DB.KGA94.5.

Dunford, R, K Michel, M Gagnage, H. Piégay, and M.-L. Trémelo. 2009. "Potential and Constraints of Unmanned Aerial Vehicle Technology for the Characterization of Mediterranean Riparian Forest." *International Journal of Remote Sensing* 30 (19): 4915–35. doi:10.1080/01431160903023025.

Erikson, Mats. 2004. *Segmentation and Classification of Individual Tree Crowns in High Spatial Resolution Aerial Image.*

Eysenrode, David Salvador-van, Jan Bogaert, Piet Van Hecke, and Ivan Impens. 1998. "Influence of Tree-Fall Orientation on Canopy Gap Shape in an Ecuadorian Rain Forest." *Journal of Tropical Ecology* 14 (6): 865–69. doi:10.1017/S0266467498000625.

Fassnacht, Fabian Ewald, Hooman Latifi, Krzysztof Sterenczak, Aneta Modzelewska, Michael Lefsky, Lars T. Waser, Christoph Straub, and Aniruddha Ghosh. 2016. "Review of Studies on Tree Species Classification from Remotely Sensed Data." *Remote Sensing of Environment* 186: 64–87. doi:10.1016/j.rse.2016.08.013.

Feng, Quanlong, Jiantao Liu, and Jianhua Gong. 2015. "UAV Remote Sensing for Urban Vegetation Mapping Using Random Forest and Texture Analysis." *Remote Sensing* 7 (1): 1074–94. doi:10.3390/rs70101074.

Flynn, Kyle F., and Steven C. Chapra. 2014. "Remote Sensing of Submerged Aquatic Vegetation in a Shallow Non-Turbid River Using an Unmanned Aerial Vehicle." *Remote Sensing* 6 (12): 12815–36. doi:10.3390/rs61212815.

ForestEurope. 2016. "SFM Criteria & Indicators - Forest Europe." *Foresteurope.org*. http://foresteurope.org/sfm-criteria-indicators2/#1472655675267-8e6b009d-b722a184-c9ce5d80-64e0.

Franklin, Jerry F, Thomas A Spies, Robert Van Pelt, Andrew B Carey, Dale A Thornburgh, Dean Rae Berg, David B Lindenmayer, et al. 2002. "Disturbances and Structural Development of Natural Forest Ecosystems with Silvicultural Implications, Using Douglas-Fir Forests as an Example." *Forest Ecology and Management* 155 (1–3): 399–423. doi:10.1016/S0378-1127(01)00575-8.

Fritz, A, T Kattenborn, and B Koch. 2013. "UAV-BASED PHOTOGRAMMETRIC POINT CLOUDS -TREE STEM MAPPING IN OPEN STANDS IN COMPARISON TO TERRESTRIAL LASER SCANNER POINT CLOUDS." *International Archives of the Photogrammetry, Remote Sensing and Spatial Information Sciences* XL-1/W2 (4 – 6 September): 141–46. https://pdfs.semanticscholar.org/86ae/6b335ab8134506234d9ebd2c9f37736fd84b.pdf.

Garbarino, Matteo, Enrico Borgogno Mondino, Emanuele Lingua, Thomas A. Nagel, Vojislav Duki?, Zoran Govedar, and Renzo Motta. 2012. "Gap Disturbances and Regeneration Patterns in a Bosnian Old-Growth Forest: A Multispectral Remote Sensing and Ground-Based Approach." *Annals of Forest Science* 69 (5). Springer-Verlag: 617–25. doi:10.1007/s13595-011-0177-9.

Garcia-Ruiz, Francisco, Sindhuja Sankaran, Joe Mari Maja, Won Suk Lee, Jesper Rasmussen, and Reza Ehsani. 2013. "Comparison of Two Aerial Imaging Platforms for Identification of Huanglongbing-Infected Citrus Trees." *Computers and Electronics in Agriculture* 91. Elsevier B.V.: 106–15. doi:10.1016/j.compag.2012.12.002.

Getzin, Stephan, Robert S. Nuske, and Kerstin Wiegand. 2014. "Using Unmanned Aerial Vehicles (UAV) to Quantify Spatial Gap Patterns in Forests." *Remote Sensing* 6 (8): 6988–7004. doi:10.3390/rs6086988.

Getzin, Stephan, Kerstin Wiegand, and Ingo Schöning. 2012. "Assessing Biodiversity in Forests Using Very High-Resolution Images and Unmanned Aerial Vehicles." *Methods in Ecology and Evolution* 3 (2): 397–404. doi:10.1111/j.2041-210X.2011.00158.x.

Gini, Rossana, Daniele Passoni, Livio Pinto, and Giovanna Sona. 2014. "Use of Unmanned Aerial Systems for Multispectral Survey and Tree Classification: A Test in a Park Area of Northern Italy." *European Journal of Remote Sensing* 47 (1): 251–69. doi:10.5721/EuJRS20144716.

Hall, R J, G Castilla, J C White, B J Cooke, and R S Skakun. 2016. "Remote Sensing of Forest Pest Damage: A Review and Lessons Learned from a Canadian Perspective." *The Canadian Entomologist* i (2016): 1–61. doi:10.4039/tce.2016.11.

Hansen, M. C., P. V. Potapov, R. Moore, M. Hancher, S. A. Turubanova, A. Tyukavina, D. Thau, et al. 2013. "High-Resolution Global Maps of 21st-Century Forest Cover Change." *Science* 342 (6160): 850–53. doi:10.1126/science.1244693.

Harwin, Steve, and Arko Lucieer. 2012. "Assessing the Accuracy of Georeferenced Point Clouds Produced via Multi-View Stereopsis from Unmanned Aerial Vehicle (UAV) Imagery." *Remote Sensing* 4 (6): 1573–99. doi:10.3390/rs4061573.

Hauke, Jan, and Tomasz Kossowski. 2011. "COMPARISON OF VALUES OF PEARSON'S AND SPEARMAN'S CORRELATION COEFFICIENTS ON THE SAME SETS OF DATA." *Quaestiones Geographicae* 30 (2): 87–93. doi:10.2478/v10117-011-0021-1.

Hobi, M. L., C. Ginzler, B. Commarmot, and H. Bugmann. 2015. "Gap Pattern of the Largest Primeval Beech Forest of Europe Revealed by Remote Sensing." *Ecosphere* 6 (5). Ecological Society of America: art76. doi:10.1890/ES14-00390.1.

Hung, Calvin, Mitch Bryson, and Salah Sukkarieh. 2012. "Multi-Class Predictive Template for Tree Crown Detection." *ISPRS Journal of Photogrammetry and Remote Sensing* 68 (1). International Society for Photogrammetry and Remote Sensing, Inc. (ISPRS): 170–83. doi:10.1016/j.isprsjprs.2012.01.009.

Hung, Calvin, Zhe Xu, and Salah Sukkarieh. 2014. "Feature Learning Based Approach for Weed Classification Using High Resolution Aerial Images from a Digital Camera Mounted on a UAV." *Remote Sensing* 6 (12): 12037–54. doi:10.3390/rs61212037.

Husson, Eva, Frauke Ecke, and Heather Reese. 2016. "Comparison of Manual Mapping and Automated Object-Based Image Analysis of Non-Submerged Aquatic Vegetation from Very-High-Resolution UAS Images." *Remote Sensing* 8 (9): 724. doi:10.3390/rs8090724.

Jaakkola, Anttoni, Juha Hyyppä, Antero Kukko, Xiaowei Yu, Harri Kaartinen, Matti Lehtomäki, and Yi Lin. 2010. "A Low-Cost Multi-Sensoral Mobile Mapping System and Its Feasibility for Tree Measurements." *ISPRS Journal of Photogrammetry and Remote Sensing* 65 (6). Elsevier B.V.: 514–22. doi:10.1016/j.isprsjprs.2010.08.002.

Jensen, Jennifer, and Adam Mathews. 2016. "Assessment of Image-Based Point Cloud Products to Generate a Bare Earth Surface and Estimate Canopy Heights in a Woodland Ecosystem." *Remote Sensing* 8 (1). Multidisciplinary Digital Publishing Institute: 50. doi:10.3390/rs8010050.

Kachamba, Daud, Ole Hans Ørka, Terje Gobakken, Tron Eid, and Weston Mwase. 2016. "Biomass Estimation Using 3D Data from Unmanned Aerial Vehicle Imagery in a Tropical Woodland." *Remote Sensing 2016, Vol. 8, Page 968* 8 (11): 968. doi:10.3390/RS8110968.

Koukoulas, S., and G. A. Blackburn. 2004. "Quantifying the Spatial Properties of Forest Canopy Gaps Using LiDAR Imagery and GIS." *International Journal of Remote Sensing* 25 (15): 3049–72. doi:10.1080/01431160310001657786.

Legendre, Pierre, and Louis Legendre. 1983. *Numerical Ecology*. Developmen. Amsterdam: Elsevier B.V. http://www.ievbras.ru/ecostat/Kiril/R/Biblio/Statistic/Legendre P., Legendre L. Numerical ecology.pdf.

Lehmann, Jan Rudolf Karl, Felix Nieberding, Torsten Prinz, and Christian Knoth. 2015. "Analysis of Unmanned Aerial System-Based CIR Images in Forestry-a New Perspective to Monitor Pest Infestation Levels." *Forests* 6 (3): 594–612. doi:10.3390/f6030594.

Li, Dong, Huadong Guo, Cheng Wang, Wang Li, Hanyue Chen, and Zhengli Zuo. 2016. "Individual Tree Delineation in Windbreaks Using Airborne-Laser-Scanning Data and Unmanned Aerial Vehicle Stereo Images." *IEEE Geoscience and Remote Sensing Letters* 13 (9): 1330–34. doi:10.1109/LGRS.2016.2584109.

Li, Manchun, Lei Ma, Thomas Blaschke, Liang Cheng, and Dirk Tiede. 2016. "A Systematic Comparison of Different Object- Based Classification Techniques Using High Spatial Resolution Imagery in Agricultural Environments." *International Journal of Applied Earth Observation and Geoinformation* 49 (April). Elsevier B.V.: 87–98. doi:10.1016/j.jag.2016.01.011.

Li, Xiaoxiao, and Guofan Shao. 2014. "Object-Based Land-Cover Mapping with High Resolution Aerial Photography at a County Scale in Midwestern USA." *Remote Sensing* 6 (11): 11372–90. doi:10.3390/rs61111372.

Lin, Chinsu, Ka-Lok Lo, and Puo-Lin Huang. 2016. "A Classification Method of Unmanned-Aerial-Systems-Derived Point Cloud for Generating a Canopy Height Model of Farm Forest." In *2016 IEEE International Geoscience and Remote Sensing Symposium (IGARSS)*, 740–43. IEEE. doi:10.1109/IGARSS.2016.7729186.

Lisein, Jonathan, Julie Linchant, Philippe Lejeune, Philippe Bouche, and Cedric Vermeulen. 2013. "Aerial Surveys Using an Unmanned Aerial System (UAS): Comparison of Different Methods for Estimating the Surface Area of Sampling Strips." *Tropical Conservation Science* 6 (4): 506–20. http://hdl.handle.net/2268/156699.

Lisein, Jonathan, Adrien Michez, Hugues Claessens, and Philippe Lejeune. 2015. "Discrimination of Deciduous Tree Species from Time Series of Unmanned Aerial System Imagery." *PLoS ONE* 10 (11): 1–20. doi:10.1371/journal.pone.0141006.

Lisein, Jonathan, Marc Pierrot-Deseilligny, Sťephanie Bonnet, and Philippe Lejeune. 2013. "A Photogrammetric Workflow for the Creation of a Forest Canopy Height Model from Small Unmanned Aerial System Imagery." *Forests* 4 (4): 922–44. doi:10.3390/f4040922.

Liu, Shao-Chong, Wen-Biao Duan, Jing Feng, and Sheng-Zhong Han. 2011. "[Effects of Forest Gap on Tree Species Regeneration and Diversity of Mixed Broadleaved Korean Pine Forest in Xiaoxing'an Mountains]." *Ying Yong Sheng Tai Xue Bao = The Journal of Applied Ecology* 22 (6): 1381–88. http://www.ncbi.nlm.nih.gov/pubmed/21941734.

Ma, Lei, Liang Cheng, Manchun Li, Yongxue Liu, and Xiaoxue Ma. 2015. "Training Set Size, Scale, and Features in Geographic Object-Based Image Analysis of Very High Resolution Unmanned Aerial Vehicle Imagery." *ISPRS Journal of Photogrammetry and Remote Sensing* 102. International Society for Photogrammetry and Remote Sensing, Inc. (ISPRS): 14–27. doi:10.1016/j.isprsjprs.2014.12.026.

Main-Knorn, Magdalena, Gretchen G. Moisen, Sean P. Healey, William S. Keeton, Elizabeth A. Freeman, and Patrick Hostert. 2011. "Evaluating the Remote Sensing and Inventory-Based Estimation of Biomass in the Western Carpathians." *Remote Sensing* 3 (7): 1427–46. doi:10.3390/rs3071427.

Meng, Ran, Jin Wu, Kathy L Schwager, Feng Zhao, Philip E Dennison, Bruce D Cook, Kristen Brewster, Timothy M Green, and Shawn P Serbin. 2017. "Using High Spatial Resolution Satellite Imagery to Map Forest Burn Severity across Spatial Scales in a Pine Barrens Ecosystem." *Remote Sensing of Environment* 191. Elsevier Inc.: 95–109. doi:10.1016/j.rse.2017.01.016.

Messinger, Max, Gregory P. Asner, and Miles Silman. 2016. "Rapid Assessments of Amazon Forest Structure and Biomass Using Small Unmanned Aerial Systems." *Remote Sensing* 8 (8): 1–15. doi:10.3390/rs8080615.

Michez, Adrien, Hervé Piégay, Jonathan Lisein, Hugues Claessens, and Philippe Lejeune. 2016. "Classification of Riparian Forest Species and Health Condition Using Multi-Temporal and Hyperspatial Imagery from Unmanned Aerial System." *Environmental Monitoring and Assessment* 188 (3). Environmental Monitoring and Assessment: 146. doi:10.1007/s10661-015-4996-2.

Mikita, Tomáš, Přemysl Janata, and Peter Surový. 2016. "Forest Stand Inventory Based on Combined Aerial and Terrestrial Close-Range Photogrammetry." *Forests* 7 (8). Multidisciplinary Digital Publishing Institute: 165. doi:10.3390/f7080165.

Møller, Anders Pape, and Michael D. Jennions. 2002. "How Much Variance Can Be Explained by Ecologists and Evolutionary Biologists?" *Oecologia* 132 (4): 492–500. doi:10.1007/s00442-002-0952-2.

Moser, Dietmar, Harald G. Zechmeister, Christoph Plutzar, Norbert Sauberer, Thomas Wrbka, and Georg Grabherr. 2002. "Landscape Patch Shape Complexity as an Effective Measure for Plant Species Richness in Rural Landscapes." *Landscape Ecology* 17 (7). Kluwer Academic Publishers: 657–69. doi:10.1023/A:1021513729205.

Moskal, L. Monika, Diane M. Styers, and Meghan Halabisky. 2011. "Monitoring Urban Tree Cover Using Object-Based Image Analysis and Public Domain Remotely Sensed Data." *Remote Sensing* 3 (10): 2243–62. doi:10.3390/rs3102243.

Muscolo, Adele, Silvio Bagnato, Maria Sidari, and Roberto Mercurio. 2014. "A Review of the Roles of Forest Canopy Gaps." *Journal of Forestry Research* 25 (4): 725–36. doi:10.1007/s11676-014-0521-7.

Muscolo, Adele, G. Settineri, S. Bagnato, R. Mercurio, and M. Sidari. 2017. "Use of Canopy Gap Openings to Restore Coniferous Stands in Mediterranean Environment." *iForest* 10 (1). SISEF - Italian Society of Silviculture and Forest Ecology: 322. doi:10.3832/IFOR1983-009.

Myers, Derek, Charles McCauley Ross, and Bo Liu. 2015. "A Review of Unmanned Aircraft System (UAS) Applications for Agriculture." *2015 ASABE International Meeting*, 1. doi:10.13031/aim.20152189593.

Näsi, Roope, E. Honkavaara, S. Tuominen, H. Saari, I. Pölönen, T. Hakala, N. Viljanen, et al. 2016. "Uas Based Tree Species Identification Using the Novel Fpi Based Hyperspectral Cameras in Visible, Nir and Swir Spectral Ranges." *International Archives of the Photogrammetry, Remote Sensing and Spatial Information Sciences - ISPRS Archives* 2016–Janua (July): 1143–48. doi:10.5194/isprsarchives-XLI-B1-1143-2016.

Näsi, Roope, Eija Honkavaara, Päivi Lyytikäinen-Saarenmaa, Minna Blomqvist, Paula Litkey, Teemu Hakala, Niko Viljanen, Tuula Kantola, Topi Tanhuanpää, and Markus Holopainen. 2015. "Using UAV-Based Photogrammetry and Hyperspectral Imaging for Mapping Bark Beetle Damage at Tree-Level." *Remote Sensing* 7 (11): 15467–93. doi:10.3390/rs71115467.

Nevalainen, Olli, Eija Honkavaara, Sakari Tuominen, Niko Viljanen, Teemu Hakala, Xiaowei Yu, Juha Hyyppä, et al. 2017. "Individual Tree Detection and Classification with UAV-Based Photogrammetric Point Clouds and Hyperspectral Imaging." *Remote Sensing* 9 (3): 185. doi:10.3390/rs9030185.

Nijland, Wiebe, Nicholas C. Coops, S. Ellen Macdonald, Scott E. Nielsen, Christopher W. Bater, and J. John Stadt. 2015. "Comparing Patterns in Forest Stand Structure Following Variable Harvests Using Airborne Laser Scanning Data." *Forest Ecology and Management* 354: 272–80. doi:10.1016/j.foreco.2015.06.005.

Nyamgeroh, Beryl. 2015. "Object Oriented Detection of Canopy Gaps From Very High Resolution Aerial Images." Faculty of Geo-Information Science and Earth Observation of the University of Twente, Netherlands. http://www.itc.nl/library/papers_2015/msc/nrm/nyamgeroh.pdf.

Oliver, C. D., and B. C. Larson. 1996. *Forest Stand Dynamics (Update Edition)*. Ohn Wiley. New York.

Ørka, Ole Hans, and M Dalponte. 2013. "Characterizing Forest Species Composition Using Multiple Remote Sensing Data Sources and Inventory Approaches." *Scandinavian Journal of Forest Research* 28 (7): 677–88. doi:10.1080/02827581.2013.793386.

Paneque-Gálvez, Jaime, Michael K. McCall, Brian M. Napoletano, Serge A. Wich, and Lian Pin Koh. 2014. "Small Drones for Community-Based Forest Monitoring: An Assessment of Their Feasibility and Potential in Tropical Areas." *Forests* 5 (6): 1481–1507. doi:10.3390/f5061481.

Pelletier, Charlotte, Silvia Valero, Jordi Inglada, Nicolas Champion, and Gérard Dedieu. 2016. "Assessing the Robustness of Random Forests to Map Land Cover with High Resolution Satellite Image Time Series over Large Areas." *Remote Sensing of Environment* 187. Elsevier Inc.: 156–68. doi:10.1016/j.rse.2016.10.010.

Perroy, Ryan L., Timo Sullivan, and Nathan Stephenson. 2017. "Assessing the Impacts of Canopy Openness and Flight Parameters on Detecting a Sub-Canopy Tropical Invasive Plant Using a Small Unmanned Aerial System." *ISPRS Journal of Photogrammetry and Remote Sensing* 125. International Society for Photogrammetry and Remote Sensing, Inc. (ISPRS): 174–83. doi:10.1016/j.isprsjprs.2017.01.018.

Pielou, E. C. 1975. *Ecological Diversity. Wiley & Sons*. New York. doi:10.1086/282439.

Popma, J., and F. Bongers. 1988. "The Effect of Canopy Gaps on Growth and Morphology of Seedlings of Rain Forest Species." *Oecologia* 75 (4). Springer-Verlag: 625–32. doi:10.1007/BF00776429.

Puissant, Anne, Simon Rougier, and André Stumpf. 2014. "Object-Oriented Mapping of Urban Trees Using Random Forest Classifiers." *International Journal of Applied Earth Observation and Geoinformation* 26. Elsevier B.V.: 235–45. doi:10.1016/j.jag.2013.07.002.

Puliti, Stefano, Hans Olerka, Terje Gobakken, and Erik Næsset. 2015. "Inventory of Small Forest Areas Using an Unmanned Aerial System." *Remote Sensing* 7 (8): 9632–54. doi:10.3390/rs70809632.

Quiros, Juan Jose, and Lav R. Khot. 2016. "Potential of Low Altitude Multispectral Imaging for in-Field Apple Tree Nursery Inventory Mapping." *IFAC-PapersOnLine* 49 (16). Elsevier B.V.: 421–25. doi:10.1016/j.ifacol.2016.10.077.

Rasmussen, Jesper, Georgios Ntakos, Jon Nielsen, Jesper Svensgaard, Robert N. Poulsen, and Svend Christensen. 2016. "Are Vegetation Indices Derived from Consumer-Grade Cameras Mounted on UAVs Sufficiently Reliable for Assessing Experimental Plots?" *European Journal of Agronomy* 74. Elsevier B.V.: 75–92. doi:10.1016/j.eja.2015.11.026.

Roth, Keely L., Dar A. Roberts, Philip E. Dennison, Seth H. Peterson, and Michael Alonzo. 2015. "The Impact of Spatial Resolution on the Classification of Plant Species and Functional Types within Imaging Spectrometer Data." *Remote Sensing of Environment* 171 (December): 45–57. doi:10.1016/j.rse.2015.10.004.

Salamí, Esther, Cristina Barrado, and Enric Pastor. 2014. "UAV Flight Experiments Applied to the Remote Sensing of Vegetated Areas." *Remote Sensing* 6 (11): 11051–81. doi:10.3390/rs61111051.

Salo, Heikki, Ville Tirronen, Ilkka Pölönen, Sakari Tuominen, Andras Balazs, Jan Heikkilä, and Heikki Saari. 2012. "Methods for Estimating Forest Stem Volumes by Tree Species Using Digital Surface Model and CIR Images Taken from Light UAS." In *SPIE 8390, Algorithms and Technologies for Multispectral, Hyperspectral, and Ultraspectral Imagery XVIII*, edited by Sylvia S. Shen and Paul E. Lewis, 83900G–83900G–6. International Society for Optics and Photonics. doi:10.1117/12.919085.

Sandbrook, Chris. 2015. "The Social Implications of Using Drones for Biodiversity Conservation." *Ambio* 44 (4). Springer Netherlands: 636–47. doi:10.1007/s13280-015-0714-0.

Saura, Santiago, and Pedro Carballal. 2004. "Discrimination of Native and Exotic Forest Patterns through Shape Irregularity Indices: An Analysis in the Landscapes of Galicia, Spain." *Landscape Ecology* 19: 647–62. http://www2.montes.upm.es/personales/saura/pdf/Lecol2004b.pdf.

Schliemann, Sarah A., and James G. Bockheim. 2011. "Methods for Studying Treefall Gaps: A Review." *Forest Ecology and Management* 261 (7). Elsevier B.V.: 1143–51. doi:10.1016/j.foreco.2011.01.011.

Scoppola, A., and C. Caporali. 1998. "Mesophilous Woods with Fagus Sylvatica L. of Northern Latium (Tyrrenian Central Italy): Synecology and Syntaxonomy." *Plant Biosystems* 132 (2): 151–68.

Seidel, Dominik, Christian Ammer, and Klaus Puettmann. 2015. "Describing Forest Canopy Gaps Efficiently, Accurately, and Objectively: New Prospects through the Use of Terrestrial Laser Scanning." *Agricultural and Forest Meteorology* 213. Elsevier B.V.: 23–32. doi:10.1016/j.agrformet.2015.06.006.

Shannon, C. 1948. "A Mathematical Theory of Communication." *Bell Syst. Tech. J.* 27: 379–423.

Singh, Minerva, Damian Evans, Boun Suy Tan, and Chan Samean Nin. 2015. "Mapping and Characterizing Selected Canopy Tree Species at the Angkor World Heritage Site in Cambodia Using Aerial Data." *PLoS ONE* 10 (4): 1–26. doi:10.1371/journal.pone.0121558.

Stumpf, André, and Norman Kerle. 2011. "Object-Oriented Mapping of Landslides Using Random Forests." *Remote Sensing of Environment* 115 (10). Elsevier Inc.: 2564–77. doi:10.1016/j.rse.2011.05.013.

Suárez, Juan C., Carlos Ontiveros, Steve Smith, and Stewart Snape. 2005. "Use of Airborne LiDAR and Aerial Photography in the Estimation of Individual Tree Heights in Forestry." *Computers and Geosciences* 31 (2): 253–62. doi:10.1016/j.cageo.2004.09.015.

Suomalainen, Juha, Niels Anders, Shahzad Iqbal, Gerbert Roerink, Jappe Franke, Philip Wenting, Dirk Hünniger, Harm Bartholomeus, Rolf Becker, and Lammert Kooistra. 2014. "A Lightweight Hyperspectral Mapping System and Photogrammetric Processing Chain for Unmanned Aerial Vehicles." *Remote Sensing* 6 (11): 11013–30. doi:10.3390/rs61111013.

Tang, Lina, and Guofan Shao. 2015. "Drone Remote Sensing for Forestry Research and Practices." *Journal of Forestry Research* 26 (4). Northeast Forestry University: 791–97. doi:10.1007/s11676-015-0088-y.

Turner, Darren, Arko Lucieer, Zbyněk Malenovský, Diana H. King, and Sharon A. Robinson. 2014. "Spatial Co-Registration of Ultra-High Resolution Visible, Multispectral and Thermal Images Acquired with a Micro-UAV over Antarctic Moss Beds." *Remote Sensing* 6 (5): 4003–24. doi:10.3390/rs6054003.

Turner, Darren, Arko Lucieer, and Luke Wallace. 2014. "Direct Georeferencing of Ultrahigh-Resolution UAV Imagery." *IEEE Transactions on Geoscience and Remote Sensing* 52 (5): 2738–45. doi:10.1109/TGRS.2013.2265295.

Turner, Darren, Arko Lucieer, and Christopher Watson. 2012. "An Automated Technique for Generating Georectified Mosaics from Ultra-High Resolution Unmanned Aerial Vehicle (UAV) Imagery, Based on Structure from Motion (SFM) Point Clouds." *Remote Sensing* 4 (5): 1392–1410. doi:10.3390/rs4051392.

Vepakomma, Udayalakshmi, Benoit St-Onge, and Daniel Kneeshaw. 2008. "Spatially Explicit Characterization of Boreal Forest Gap Dynamics Using Multi-Temporal Lidar Data." *Remote Sensing of Environment* 112 (5): 2326–40. doi:10.1016/j.rse.2007.10.001.

Wallace, Luke, Arko Lucieer, Zbynek Malenovsky, Darren Turner, and Petr Vopenka. 2016. "Assessment of Forest Structure Using Two UAV Techniques: A Comparison of Airborne Laser Scanning and Structure from Motion (SfM) Point Clouds." *Forests* 7 (3): 1–16. doi:10.3390/f7030062.

Wallace, Luke, Arko Lucieer, Christopher Watson, and Darren Turner. 2012. "Development of a UAV-LiDAR System with Application to Forest Inventory." *Remote Sensing* 4 (12). Molecular Diversity Preservation International: 1519–43. doi:10.3390/rs4061519.

Wallace, Luke, Robert Musk, and Arko Lucieer. 2014. "An Assessment of the Repeatability of Automatic Forest Inventory Metrics Derived from UAV-Borne Laser Scanning Data." *IEEE Transactions on Geoscience and Remote Sensing* 52 (11): 7160–69. doi:10.1109/TGRS.2014.2308208.

Wallace, Luke, Christopher Watson, and Arko Lucieer. 2014. "Detecting Pruning of Individual Stems Using Airborne Laser Scanning Data Captured from an Unmanned Aerial Vehicle." *International Journal of Applied Earth Observation and Geoinformation* 30 (1). Elsevier B.V.: 76–85. doi:10.1016/j.jag.2014.01.010.

Watts, Adam C., Vincent G. Ambrosia, and Everett A. Hinkley. 2012. "Unmanned Aircraft Systems in Remote Sensing and Scientific Research: Classification and Considerations of Use." *Remote Sensing* 4 (6): 1671–92. doi:10.3390/rs4061671.

Whitehead, Ken, and Chris H. Hugenholtz. 2014. "Remote Sensing of the Environment with Small Unmanned Aircraft Systems (UASs), Part 1: A Review of Progress and Challenges 1." *Journal of Unmanned Vehicle Systems* 2 (3): 69–85. doi:10.1139/juvs-2014-0006.

Yang, Jian, Trevor Jones, John Caspersen, and Yuhong He. 2015. "Object-Based Canopy Gap Segmentation and Classification : Quantifying the Pros and Cons of Integrating Optical and LiDAR Data." *Remote Sensing* 7 (12): 15917–32. doi:10.3390/rs71215811.

Zahawi, Rakan A., Jonathan P. Dandois, Karen D. Holl, Dana Nadwodny, J. Leighton Reid, and Erle C. Ellis. 2015. "Using Lightweight Unmanned Aerial Vehicles to Monitor Tropical Forest Recovery." *Biological Conservation* 186. Elsevier Ltd: 287–95. doi:10.1016/j.biocon.2015.03.031.

Zarco-Tejada, P. J., R. Diaz-Varela, V. Angileri, and P. Loudjani. 2014. "Tree Height Quantification Using Very High Resolution Imagery Acquired from an Unmanned Aerial Vehicle (UAV) and Automatic 3D Photo-Reconstruction Methods." *European Journal of Agronomy* 55. Elsevier B.V.: 89–99. doi:10.1016/j.eja.2014.01.004.

Zhang, H, and Chi Yung Jim. 2013. "Species Adoption for Sustainable Forestry in Hong Kong's Degraded Countryside." *International Journal of Sustainable Development & World Ecology* 20 (6): 484–503. doi:Doi 10.1080/13504509.2013.818590.

Zhang, Jian, Jianbo Hu, Juyu Lian, Zongji Fan, Xuejun Ouyang, and Wanhui Ye. 2016. "Seeing the Forest from Drones: Testing the Potential of Lightweight Drones as a Tool for Long-Term Forest Monitoring." *Biological Conservation* 198. Elsevier Ltd: 60–69. doi:10.1016/j.biocon.2016.03.027.

Zhang, Jian, Scott E. Nielsen, Lingfeng Mao, Shengbin Chen, and Jens Christian Svenning. 2016. "Regional and Historical Factors Supplement Current Climate in Shaping Global Forest Canopy Height." *Journal of Ecology* 104 (2): 469–78. doi:10.1111/1365-2745.12510.

Zhang, Kongwen, and Baoxin Hu. 2012. "Individual Urban Tree Species Classification Using Very High Spatial Resolution Airborne Multi-Spectral Imagery Using Longitudinal Profiles." *Remote Sensing* 4 (12). Molecular Diversity Preservation International: 1741–57. doi:10.3390/rs4061741.

Zhang, Yongjun, Jinxin Xiong, and Lijuan Hao. 2011. "Photogrammetric Processing of Low-Altitude Images Acquired by Unpiloted Aerial Vehicles." *Photogrammetric Record* 26 (134): 190–211. doi:10.1111/j.1477-9730.2011.00641.x.

Zhen, Zhen, Lindi J. Quackenbush, and Lianjun Zhang. 2016. "Trends in Automatic Individual Tree Crown Detection and Delineation-Evolution of LiDAR Data." *Remote Sensing* 8 (4): 1–26. doi:10.3390/rs8040333.

Zielewska-Büttner, Katarzyna, Petra Adler, Michaela Ehmann, and Veronika Braunisch. 2016a. "Automated Detection of Forest Gaps in Spruce Dominated Stands Using Canopy Height Models Derived from Stereo Aerial Imagery." *Remote Sensing* 8 (3): 1–21. doi:10.3390/rs8030175.

———. 2016b. "Automated Detection of Forest Gaps in Spruce Dominated Stands Using Canopy Height Models Derived from Stereo Aerial Imagery." *Remote Sensing* 8 (3): 1–21. doi:10.3390/rs8030175.

Zielewska-Büttner, Katarzyna, Petra Adler, Maike Petersen, and Veronika Braunisch. 2016. "Parameters Influencing Forest Gap Detection Using Canopy Height Models Derived From Stereo Aerial Imagery." *Publikationen Der DGPF* 25: 405–16.